MOLPHARM/2005/15669

Design of PAP-1, a Selective Small Molecule Kv1.3 Blocker, for the

Suppression of Effector Memory T Cells in Autoimmune Diseases

Alexander Schmitz[1]*, Ananthakrishnan Sankaranarayanan[2]*, Philippe Azam[2], Kristina Schmidt-Lassen[1], Daniel Homerick[2], Wolfram Hänsel[1], Heike Wulff[2]

[1]*Pharmaceutical Institute, University of Kiel, 24118 Kiel, Germany*

[2]*Department of Medical Pharmacology and Toxicology, University of California, Davis, Davis, CA 95615, USA*

These authors contributed equally to this work.

Running Title: PAP-1, a selective small molecule Kv1.3 blocker

Corresponding author: Heike Wulff, Department of Medical Pharmacology and Toxicology, Genome and Biomedical Sciences Facility, Room 3502, 451 East Health Sciences Drive, University of California, Davis, Davis, CA 95616; phone: 530-754-6136; email: hwulff@ucdavis.edu

Number of Text Pages:

Number of Tables: 1

Number of Figures: 5

Number of References: 52

Number of Words in the Abstract: 250

Number of Words in the Introduction: 788

Number of Words in the Discussion: 992

Nonstandard abbreviations used: 5-MOP: 5-methoxypsoralen; DTH: delayed type hypersensitivity; K_{Ca}: Ca^{2+}-activated K^+ channel; K_v: voltage-gated K^+ channel; PAP: phenoxyalkoxypsoralen; ShK: *Stichodactyla helianthus* toxin; $[^3H]$-TdR: tritiated thymidine.

Abstract

The lymphocyte K^+ channel Kv1.3 constitutes an attractive pharmacological target for the selective suppression of terminally differentiated effector memory T (T_{EM}) cells in T-cell mediated autoimmune diseases such as multiple sclerosis and type-1 diabetes. Unfortunately, all of the existing small molecule Kv1.3 blockers are not selective and many of them like correolide, PAC and our own compound Psora-4 inhibit the cardiac K^+ channel Kv1.5. By further exploring the structure-activity relationship around Psora-4 through a combination of classical medicinal chemistry and whole-cell patch-clamp we identified a series of new phenoxyalkoxypsoralens, which exhibit 2 to 50-fold selectivity for Kv1.3 over Kv1.5 depending on their exact substitution pattern. The most potent and "drug-like" compound of this series, 5-(4-phenoxybutoxy)psoralen (PAP-1), blocks Kv1.3 in a use-dependent manner with a Hill coefficient of 2 and an EC_{50} of 2 nM by preferentially binding to the C-type inactivated state of the channel. PAP-1 is 23-fold selective over Kv1.5, 33 to 125-fold selective over other Kv1-family channels and 500 to 7500-fold selective over Kv2.1, Kv3.1, Kv3.2, Kv4.2, HERG, calcium-activated K^+ channels, Na^+, Ca^{2+} and Cl^- channels. PAP-1 does not exhibit cytotoxic or phototoxic effects, is negative in the Ames test and affects P450-dependent enzymes only at micromolar concentrations. PAP-1 potently inhibits the proliferation of human T_{EM} cells and suppresses delayed type hypersensitivity, a T_{EM} cell mediated reaction, in rats. PAP-1 and several of its derivatives therefore constitute excellent new tools to further explore Kv1.3 as a target for immunosuppression and could potentially be developed into orally available immunomodulators.

Introduction

Potassium (K$^+$) channels in humans are encoded by an extended super-family of 76 genes (Gutman et al., 2003). Each K$^+$ channel has a unique expression pattern allowing cells to "fine tune" their membrane potential and their excitability according to their respective functions. Specific K$^+$ channel modulation therefore offers an enormous potential for the development of new drugs. One channel that constitutes an especially promising target is the voltage-gated Kv1.3 channel. Homomeric Kv1.3 channels are found in human T and B lymphocytes and their expression is up-regulated in terminally differentiated effector memory T cells (Wulff et al., 2003b) and class-switched memory B cells (Wulff et al., 2004). Kv1.3 blockers have therefore been proposed as potential new therapeutics for the treatment of autoimmune diseases such as multiple sclerosis, type-1 diabetes, psoriasis, rheumatoid arthritis, transplant rejection, graft-versus-host disease, Sjorgen's Syndrom and systemic lupus erythematosus, where effector memory T cells and/or class-switched memory B cells are involved in the pathogenesis (Dorner and Lipsky, 2004; Fasth et al., 2004; Hansen et al., 2002; Markovic-Plese et al., 2001; Pearl et al., 2005; Viglietta et al., 2002; Vissers et al., 2004; Wulff et al., 2003b; Yamashita et al., 2004). In proof of this hypothesis the Kv1.3 blocking peptides kaliotoxin (Beeton et al., 2001a), ShK (Beeton et al., 2001b) and its recently identified more specific derivative ShK(L5) (Beeton et al., 2005) have been shown to treat experimental autoimmune encephalomyelitis, an animal model for multiple sclerosis (MS). Kv1.3 has been further validated as a target for the treatment of MS by the demonstration that myelin-reactive T cells in the blood from patients with MS are predominantly Kv1.3^{high} effector memory T cells (Wulff et al., 2003b). Contrary to the aforementioned peptides a small molecule Kv1.3 blocker would have the advantage that it could be taken orally.

The first small molecules that were found to inhibit the Kv channel in human T cells were the classical Kv channel inhibitors 4-aminopyridine and tetraethylammonium, the Ca^{2+}-activated K^+ channel blocker quinine and the Ca^{2+} channel inhibitors verapamil, diltiazem and nifedipine (for recent reviews see: (Chandy et al., 2004; Wulff et al., 2003a)). Following the cloning of the *Kv1.3* gene in the early 1990s (Grissmer et al., 1990), several pharmaceutical companies started screening their libraries for more potent and more selective small molecule Kv1.3 blockers and identified a number of compound classes that roughly fall into two groups: 1. Typical combinatorial library compounds like the iminodihydroquinoline CP-339818 (Nguyen et al., 1996), the benzylpiperidine UK-78282 (Hanson et al., 1999), the cyclohexyl-substituted benzamides (Schmalhofer et al., 2002) and the sulfamidebenzamidoindanes (Wulff et al., 2003a) that are of a relatively simple structure and low molecular weight and rich in nitrogen and halogen atoms; 2. Natural products or natural product-derivatives like the triterpenoid correolide (Hanner et al., 1999) and the candelalides (Singh et al., 2001) that are rich in oxygen atoms and have a more complex stereochemistry. Although some of these compounds are quite potent Kv1.3 blockers with EC_{50} values of 30-200 nM, they all lack the required selectivity over other ion channels, especially the closely related Kv1-family channels.

In contrast to the high-throughput screening approaches applied by pharmaceutical companies we took an approach that is termed "retroactive exploitation of observations made in man" (Wermuth, 2004). Following up on anecdotal reports that tea prepared from the leaves of *Ruta graveolens,* the Common Rue (Herb of Grace), alleviated the symptoms of MS (Bohuslavizki et al., 1993) we extracted *Ruta* and identified a number of Kv1-family channel blocking psoralens and furoquinolines in this plant (Bohuslavizki et al., 1994). In subsequent single case "off label" trials the psoralen 5-MOP (5-methoxypsoralen, Figure 1A), one of the

major K$^+$ channel blocking principles of *Ruta* (Bohuslavizki et al., 1994), was found to improve

the functional deficits in MS patients (Bohuslavizki et al., 1993), but its phototoxic activity and

its low affinity to Kv1.3 precluded its use as a therapeutic for MS. We therefore started a

classical medicinal chemistry program to improve the potency and selectivity of the psoralens for

Kv1.3 and identified 5,8-diethoxypsoralen (EC$_{50}$ 10 μM) (Wulff et al., 1998), 6-(2,5-

dimethoxyphenyl)psoralen (EC$_{50}$ 700 nM) (Wernekenschnieder et al., 2004) and Psora-4 (EC$_{50}$ 3

nM) (Vennekamp et al., 2004). Psora-4 (Figure 1A), our most potent compound, was 17-70-fold

selective for Kv1.3 over other Kv1-family channels with the exception of the cardiac channel

Kv1.5 (EC$_{50}$ ~8 nM) raising concerns about potential side-effects *in vivo*.

In the present study we describe how we have used Psora-4 as a template and have

successfully separated the affinities for Kv1.3 and Kv1.5 through further derivatization. Our new

psoralen Kv1.3 blocker, PAP-1, exhibits 23-fold selectivity over Kv1.5, potently suppresses the

proliferation of human T$_{EM}$ cells *in vitro* and prevents delayed type hypersensitivity (DTH) in

rats when administered intraperitoneally or orally.

Materials and Methods

Chemistry: 5-MOP was purchased from Aldrich and dealkylated with magnesium and iodine at 165°C (Schoenberg and Aziz, 1953) to obtain 5-hydroxypsoralen (5-HOP).

General method A: 5-HOP was reacted with the respective alkyl halides in the presence of an excess of anhydrous potassium carbonate and catalytic amounts of potassium iodide under reflux in a dry organic solvent. The progress of the reaction was monitored by thin layer chromatography. After completion of the reaction the crude product mixture was diluted with water and acidified to pH 1 with concentrated hydrochloric acid. The aqueous slurry was extracted with dichloromethane. The organic phase was washed first with 1% sodium hydroxide to separate the un-reacted 5-HOP and then with acidic water before it was dried over anhydrous sodium sulfate and concentrated to dryness. The resulting residue was decolorized with charcoal and re-crystallized.

General method B: 5-HOP was alkylated with 4-chloroiodobutane in dry acetone in the presence of an excess of potassium carbonate for 24-28 h at 25°C. After completion of the reaction, the product, 5-(4-chlorobutoxy)psoralen, was isolated according to General Method A and then reacted with mercapto, amino and hydroxy substituted heteroaromatics or with substituted phenols to obtain the hetero-aromatic and phenoxy substituted compounds shown in Figures 1B and 2.

General method C: To obtain phenoxy-substituted alkyl halides as reactants for General Method A, elemental sodium was stirred in 120 ml of dry ethyl alcohol and an equivalent amount of the phenol component was added drop-wise. After addition of an excess of 1,4-dibromobutane the reaction mixture was refluxed for 4 h. The solvent was evaporated, the residue dissolved in 6%

sodium hydroxide solution and extracted with ether. The organic layer was dried over sodium

sulfate and evaporated to obtain the crude product.

All newly synthesized compounds were characterized by melting point, ^{1}H and ^{13}C NMR, mass

spectrometry and combustion analysis. [13]C data is given only for PAP-1 and for PAP-17 and

PAP-17a, where it was necessary to determine the structure of the two reaction products. It is

available upon request for other compounds.

5-(4-Chlorobutoxy)psoralen (I-1). 5-HOP (817 mg, 4.0 mmol), 4-chlorobutyl iodide (1.4 g, 6.4

mmol) and potassium carbonate (3.0 g) were stirred at 25°C in 80 ml of acetone for 30 h. After

completion of the reaction the acetone was evaporated and the resulting residue suspended in

petroleum ether, filtered to separate the excess 4-chlorobutyl iodide and dried under suction

(1.10 g, 92.9%): m.p. = 115.6^{o}C; ^{1}H-NMR (500 MHz, CDCl$_3$): δ [ppm] = 8.15 (d, 1H, ^3J = 9.8

Hz, 3-H), 7.60 (d, 1H, ^3J = 2.6 Hz, 5'-H), 7.17 (s, 1H, 8-H), 6.95 (d, 1H, ^3J = 2.2 Hz, 4'-H), 6.29

(d, 1H, ^3J = 9.8 Hz, 4-H), 4.52 (t, 2H, ^3J = 5.5 Hz, 5-OC$\underline{H}_2$CH$_2$CH $_2$CH$_2$Cl), 3.68 (t, 2H, ^3J = 5.8

Hz, 5-OCH$_2$CH$_2$CH$_2$C$\underline{H}_2$Cl), 2.08 (p, 4H, ^3J = 3.0 Hz, 5-OCH$_2$C$\underline{H}_2$C$\underline{H}_2$CH$_2$Cl).

5-(3-Cyanopropoxy)psoralen (ACP-1). 5-HOP (800 mg, 3.9 mmol), 4-chlorobutyronitrile

(655.5 mg, 6.3 mmol) and potassium carbonate (2.6 g) were refluxed in 50 ml of 2-butanone for

48 h. The crude product was re-crystallized from methanol (710 mg, 66.7%): m.p. = 155.2^{o}C;

^{1}H-NMR (500 MHz, CDCl$_3$): δ [ppm] = 8.13 (d, 1H, ^3J = 9.8 Hz, 3-H), 7.63 (d, 1H, ^3J = 2.0 Hz,

5'-H), 7.21 (s, 1H, 8-H), 6.98 (d, 1H, ^3J = 2.0 Hz, 4'-H), 6.32 (d, 1H, ^3J = 9.5 Hz, 4-H), 4.58 (t,

2H, ^3J = 5.8 Hz, 5-OC$\underline{H}_2$CH$_2$CH$_2$CN), 2.72 (t, 2H, ^3J = 5.7 Hz, 5-OCH$_2$CH$_2$C$\underline{H}_2$CN), 2.26 (p,

2H, ^3J = 6.3 Hz, 5-OCH$_2$C$\underline{H}_2$CH$_2$CN); MS (70 eV) m/z: 269 (100%, M$^+$), 202 (74%,

[C$_{11}$H$_6$O$_4$]$^+$), 174 (63%, [202-CO]$^+$), 145 (26%), 118 (7%), 89 (14%); Calculated for C$_{15}$H$_{11}$NO$_4$

(269.26): C, 66.91%; H, 4.12%; N, 5.01%; O, 23.77%. Found: C, 66.52%; H, 4.03%; N, 5.01%.

5-(4-Pentynyloxy)psoralen (AP-1). 5-HOP (500 mg, 2.4 mmol), 5-chloro-1-pentyne (405.8 mg, 3.9 mmol) and potassium carbonate (2.0 g) were refluxed in 30 ml of acetonitrile for 24 h. The crude product was re-crystallized from methanol (55 mg, 8.3%): m.p. = 145.1^{o}C: ^{1}H-NMR (500 MHz, CDCl$_3$): δ [ppm] = 8.16 (d, 1H, ^3J = 9.8 Hz, 3-H), 7.60 (d, 1H, ^3J = 2.3 Hz, 5'-H), 7.17 (s, 1H, 8-H), 7.01 (d, 1H, ^3J = 1.5 Hz, 4'-H), 6.29 (d, 1H, ^3J = 9.8 Hz, 4-H), 4.56 (t, 2H, ^3J = 6.1 Hz, 5-OC$\underline{H}_2$CH$_2$CH$_2$C≡CH), 2.51 (q, 2H, ^3J = 2.6 Hz, 5-OCH$_2$CH$_2$C$\underline{H}_2$C≡CH), 2.09 (p, 2H, ^3J = 6.5 Hz, 5-OCH$_2$C$\underline{H}_2$CH$_2$C≡CH), 2.03 (t, 1H, ^4J = 2.6 Hz, 5-OCH$_2$CH$_2$CH$_2$C≡C$\underline{H}$); MS (70 eV) m/z: 268 (88%, M$^+$), 203 (15%), 202 (100%, [C$_{11}$H$_6$O$_4$]$^+$), 175 (8%), 174 (11%, [202-CO]$^+$), 173 (14%), 146 (7%), 145 (21%), 118 (8%), 89 (10%), 67 (5%, C$_5$H$_7$); Calculated for C$_{16}$H$_{12}$O$_4$ (268.27): C, 71.64%; H, 4.51%; O, 23.86%. Found: C, 71.25%; H, 4.38%; LogP: 2.88.

5-[4-(1-*N*-Pyrazolyl)butoxy]psoralen (PH-1). 5-HOP (500 mg, 2.4 mmol), 4-iodo-1-chlorobutane (893 mg, 4.1 mmol) and potassium carbonate (2.0 g) were stirred at 25°C in 30 ml of acetone for 28 h. After completion of the reaction the solvent was evaporated and the resulting residue refluxed for 50 h with pyrazole (400 mg, 5.9 mmol) and potassium carbonate (2.0 g) in 30 ml of 2-butanone. The crude product was re-crystallized from an ethyl acetate/petroleum ether mixture (20:80) to yield white crystals (108 mg, 13.5%): m.p. = 145.6^{o}C; ^{1}H-NMR (500 MHz, DMSO-d$_6$): δ [ppm] = 8.17 (d, 1H, ^3J = 9.1 Hz, 3-H), 8.02 (s, 1H, 5'-H), 7.74 (s, 1H, 5-OCH$_2$CH$_2$CH$_2$CH$_2$C$_3$$\underline{H}_3N_2$), 7.43 (s, 1H, 5-OCH$_2CH_2CH_2CH_2C_3$$\underline{H}_3N_2$), 7.34 (s, 1H, 8-H), 7.29 (s, 1H, 4'-H), 6.32 (d, 1H, ^3J = 9.1 Hz, 4-H), 4.47 (s, 2H, 5-OC$\underline{H}_2$CH$_2$CH$_2$CH$_2$C$_3$H$_3$N$_2$), 4.20 (s, 2H, 5-OCH$_2$CH$_2$CH$_2$C$\underline{H}_2$C$_3$H$_3$N$_2$), 2.0 (s, 4H, 5-OCH$_2$C$\underline{H}_2$C$\underline{H}_2$CH$_2$C$_3$H$_3$N$_2$), 1.75 (s, 2H, 5-OCH$_2$CH$_2$C$\underline{H}_2$CH$_2$C$_3$H$_3$N$_2$); MS (70 eV) m/z : 324 (29%, M$^+$), 202 (6%, [C$_{11}$H$_6$O$_4$]$^+$), 174 (6%, [202-CO]$^+$), 123 (99%), 81 (26%), 69 (13%); Calculated for C$_{18}$H$_{16}$N$_2$O$_4$(324.34): C, 66.66%; H, 4.97%; N, 8.64%; O, 19.73%. Found: C, 66.53%; H, 4.96%; N, 8.56%; LogP: 2.42.

5-[4-*N*-(4-Pyridinyl)aminobutoxy]psoralen (PH-3). 5-(4-Chlorobutoxy)psoralen (390 mg, 1.3 mmol) and 4-aminopyridine (628 mg, 6.7 mmol) were refluxed in 20 ml of acetonitrile for 45 h. The crude product was re-crystallized from 2% acidic acetone (172 mg, 30.4%): m.p. = 133.9°C; ^{1}H-NMR (500 MHz, DMSO-d$_6$): δ [ppm] = 8.27 (s, 1H, 5-OCH$_2$CH$_2$CH$_2$CH$_2$N$\underline{H}$C$_5$H$_4$N), 8.25 (d, 2H, ^3J = 7.41 Hz, 5-OCH$_2$CH$_2$CH$_2$CH$_2$NHC$_5\underline{H}_4$N), 8.18 (d, 1H, ^3J = 9.8 Hz, 3-H), 8.05 (d, 1H, ^3J = 2.6 Hz, 5'-H), 7.36 (s, 1H, 8-H), 7.33 (d, 1H, ^3J = 2.3 Hz, 4'-H), 6.85 (d, 2H, ^3J = 7.3 Hz, 5-OCH$_2$CH$_2$CH $_2$CH$_2$NHC$_5\underline{H}_4$N), 6.32 (d, 1H, ^3J = 9.8 Hz, 4-H), 4.52 (t, 2H, ^3J = 6.1 Hz, 5-OC$\underline{H}_2$CH$_2$CH$_2$CH$_2$NHC$_5$H$_4$N), 4.22 (t, 2H, ^3J = 7.0 Hz, 5-OCH$_2$CH$_2$CH$_2$C$\underline{H}_2$NHC$_5$H$_4$N), 1.99 (p, 2H, 5-OCH$_2$C$\underline{H}_2$CH$_2$CH$_2$NHC$_5$H$_4$N), 1.77 (p, 2H, 5-OCH$_2$CH$_2$C$\underline{H}_2$CH$_2$NHC$_5$H$_4$N); MS (70 eV) m/z: 350 (12%, M$^+$), 202 (99%, [C$_{11}$H$_6$O$_4$]$^+$), 174 (60%, [202-CO]$^+$), 184 (20%), 145 (11%), 123 (15%), 107 (46%), 94 (7%, C$_5$H$_6$N$_2$); Calculated for C$_{20}$H$_{18}$N$_2$O$_4$ as dihydrochloride salt (423.38): C, 56.68%; H, 4.72%; N, 6.61%; O, 18.27%. Found: C, 56.69%; H, 4.84%; N, 6.58%; Log P: 1.79.

5-[4-(5-Methyl-1,3,4-thiadiazol-2-thiolyl)butoxy]psoralen (PH-4). 5-(4-Chlorobutoxy)psoralen (500 mg, 1.7 mmol), 2-mercapto-1,3,4-thiadiazole (361 mg, 2.7 mmol) and potassium carbonate (2.0 g) were refluxed in 30 ml of 2-butanone for 66 h. The oily residue was re-crystallized from a petroleum ether/ethyl acetate (80:20) mixture (107 mg, 16.13%): m.p. = 92.1°C; ^{1}H-NMR (500 MHz, CDCl$_3$): δ [ppm] = 8.15 (d, 1H, ^3J = 9.8 Hz, 3-H), 7.59 (d, 1H, ^3J = 2.5 Hz, 5'-H), 7.16 (s, 1H, 8-H), 6.95 (d, 1H, ^3J = 2.5 Hz, 4'-H), 6.29 (d, 1H, ^3J = 9.8 Hz, 4-H), 4.51 (t, 2H, ^3J = 5.8 Hz, 5-OC$\underline{H}_2$CH$_2$CH$_2$CH$_2$S-), 3.43 (t, 2H, ^3J = 6.9 Hz, 5-OCH$_2$CH$_2$CH$_2$C$\underline{H}_2$S-), 2.74 (s, 3H, 5''-CH$_3$), 2.09 (m, 4H, ^3J = 3.0 Hz, 5-OCH$_2$C$\underline{H}_2$C$\underline{H}_2$CH$_2$S-); MS (70 eV) m/z: 388 (62%, M$^+$), 202 (14%, [C$_{11}$H$_6$O$_4$]$^+$), 187 (96%, C$_7$H$_{11}$N$_2$S$_2$), 174 (12%, [202-CO]$^+$), 145 (10%), 133 (32%), 99 (34%, C$_3$H$_3$N$_2$S), 87 (8%, C$_4$H$_7$S), 55 (28%, C$_4$H$_7$);

Calculated for $C_{18}H_{16}N_2O_4S_2$ (388.47): C, 55.65%, H, 4.15%; N, 7.21%; O, 16.47%; S, 16.51%.

Found: C, 55.44%; H, 4.15%; N, 7.39%; S, 16.77%; Log P: 2.85.

5-[4-(7-Coumarinyloxy)butoxy]psoralen (PH-5). 5-(4-Chlorobutoxy)psoralen (500 mg, 1.7

mmol), 7-hydroxycoumarin (443 mg, 2.7 mmol) and potassium carbonate (2.0 g) were refluxed

in 30 ml of 2-butanone for 68 h. The oily residue obtained was re-crystallized from a

methanol/acetone (70:30) mixture (134 mg, 18.8%): m.p. = 147°C; ^{1}H-NMR (500 MHz, CDCl$_3$):

δ [ppm] = 8.15 (d, 1H, ^3J = 9.8 Hz, 3-H), 7.64 (d, 1H, ^3J = 9.5 Hz, 5-

OCH$_2$CH$_2$CH$_2$CH$_2$OC$_9$$\underline{H}$$_5O_2$), 7.61 (d, 1H, ^3J = 2.1 Hz, 5'-H), 7.36 (dd, 1H, ^3J = 8.6 Hz, ^5J = 2.5

Hz, 5-OCH$_2$CH$_2$CH$_2$CH$_2$OC$_9$$\underline{H}$$_5O_2$), 7.16 (s, 1H, 8-H), 6.99 (d, 1H, ^3J = 2.1 Hz, 4'-H), 6.83 (m,

2H, 5-OCH$_2$CH$_2$CH$_2$CH$_2$OC$_9$$\underline{H}$$_5O_2$), 6.26 (d, 1H, ^3J = 9.5 Hz, 4-H), 6.20 (d, 1H, ^3J = 9.8 Hz, 5-

OCH$_2$CH$_2$CH$_2$CH$_2$OC$_9$$\underline{H}$$_5O_2$), 4.57 (t, 2H, ^3J = 5.4 Hz, 5-OC$\underline{H}$$_2CH_2CH_2CH_2OC_9H_5O_2$), 4.15 (t,

2H, ^3J = 5.0 Hz, 5-OCH$_2$CH$_2$CH$_2$C$\underline{H}$$_2OC_9H_5O_2$), 2.11 (m, 4H, ^3J = 2.6 Hz, 5-

OCH$_2$C$\underline{H}$$_2C\underline{H}$$_2CH_2OC_9H_5O_2$); MS (70 eV) m/z : 418 (34%, M$^+$), 378 (68%), 217 (89%), 202

(20%, [C$_{11}$H$_6$O$_4$]$^+$), 175 (100%), 174 (14%, [202-CO]$^+$), 187 (16%), 145 (32%), 134 (26%), 89

(30%), 55 (48%, C$_4$H$_7$); Calculated for C$_{24}$H$_{18}$O$_7$ (418.41) C, 68.90%; H, 4.34%; O, 26.77%.

Found: C, 69.08%, H, 4.46%; LogP: 3.34.

5-[4-(5-Methoxy-1,3-benzothiazol-2-thiolyl)butoxy]psoralen (PH-8). 2-Mercapto-5-methoxy-

1,3-benzothiazole (539 mg, 2.7 mmol) and potassium hydroxide (161 mg, 2.8 mmol) were

refluxed in 25 ml of methanol untill the solution was clear. The solution was then concentrated to

dryness under vacuum to obtain the dry potassium salt. To this potassium salt was added 20 ml

of anhydrous acetonitrile, 5-(4-chlorobutoxy)psoralen (500 mg, 1.7 mmol), and sodium iodide

(333 mg, 2.2 mmol) and the resulting mixture refluxed for 69 h. The oily residue was re-

crystallized from a petroleum ether/acetone (80:20) mixture (600 mg, 48.8%): m.p. = 134.8°C;

11

^{1}H-NMR (500 MHz, CDCl$_3$): δ [ppm] = 8.09 (d, 1H, ^3J = 9.8 Hz, 3-H), 7.61 (d, 1H, ^3J = 8.9 Hz, benzothiazole), 7.58 (d, 1H, ^3J = 2.3 Hz, 5'-H), 7.35 (d, 1H, ^4J = 2.2 Hz, benzothiazole), 7.14 (s, 1H, 8-H), 6.97 (dd, 1H, ^3J = 8.9 Hz , ^4J = 2.1 Hz, benzothiazole), 6.95 (d, 1H, ^3J = 2.8 Hz, 4'-H), 6.18 (d, 1H, ^3J = 9.8 Hz, 4-H), 4.53 (t, 2H, ^3J = 5.8 Hz, 5-OC$\underline{H}_2$CH$_2$CH$_2$CH$_2$S-), 3.87 (s, 3H, O-C$\underline{H}_3$), 3.48 (t, 2H, ^3J = 6.6 Hz, 5-OCH$_2$CH$_2$CH$_2$C$\underline{H}_2$S-), 2.11 (m, 4H, 5-OCH$_2$C$\underline{H}_2$C$\underline{H}_2$CH$_2$S-); MS (70 eV) m/z: 455 (6%, M$^+$), 453 (44%), 328 (28%), 252 (100%, C$_{12}$H$_{14}$NOS$_2$), 201 (6%), 196 (12%, C$_8$H$_6$NOS$_2$), 174 (14%, [202-CO]$^+$), 145 (8%), 89 (6%), 55 (28%, C$_4$H$_7$); Calculated for C$_{23}$H$_{19}$NO$_5$S$_2$ (455.56): C, 60.70%; H, 4.65%; N, 3.07%; O, 17.64%; S, 14.08%. Found: C, 60.70%; H, 4.59%; N, 3.09%; S, 13.94%; LogP: 4.36.

5-[4-(Pyrimidin-2-thiolyl)butoxy]psoralen (PH-9). 2-Mercaptopyrimidine (306 mg, 2.7 mmol) and potassium hydroxide (163 mg, 2.8 mmol) were refluxed in 50 ml methanol untill the solution was clear. The solution was then concentrated to dryness under reduced pressure to obtain the potassium salt. To the potassium salt was added 30 ml of acetonitrile, 5-(4-chlorobutoxy)psoralen (500 mg, 1.7 mmol) and sodium iodide (333 mg 2.2 mmol) and the mixture refluxed for 67 h. The oily residue was re-crystallized from methanol (244 mg, 38.78%): m.p. = 107.1°C; ^{1}H-NMR (500 MHz, CDCl$_3$): δ [ppm] = 8.51 (d, 2H, pyrimidine), 8.14 (d, 1H, ^3J = 10.1 Hz, 3-H), 7.59 (d, 1H, ^3J = 2.4 Hz, 5'-H), 7.16 (s, 1H, 8-H), 7.0 (t, 1H, ^3J = 4.9 Hz, pyrimidine), 6.96 (d, 1H, ^3J = 1.5 Hz, 4'-H), 6.25 (d, 1H, ^3J = 9.8 Hz, 4-H), 4.52 (t, 2H, ^3J = 5.8 Hz, 5-OC$\underline{H}_2$CH$_2$CH$_2$CH$_2$S-), 3.29 (t, 2H, ^3J = 6.8 Hz, 5-OCH$_2$CH$_2$CH$_2$C$\underline{H}_2$S-), 2.01 (m, 4H, 5-OCH$_2$C$\underline{H}_2$C$\underline{H}_2$CH$_2$S-); MS (70 eV) m/z: 368 (27%, M$^+$), 202 (8%, [C$_{11}$H$_6$O$_4$]$^+$), 167 (100%, C$_8$H$_{11}$N$_2$S), 125 (34%), 113 (37%), 55 (26%, C$_4$H$_7$); Calculated for C$_{19}$H$_{16}$N$_2$O$_4$S (368.41): C, 61.94%; H, 4.38%; N, 7.60%; O, 17.37%; S, 8.70%. Found: C, 61.85%; H, 4.34%; N, 7.41%; S, 8.66%; LogP: 3.00.

5-[4-(*N*-Phthalimido)butoxy]psoralen (PP-1). 5-HOP (500 mg, 2.5 mmol), *N*-(4-bromobutyl)phthalimide (1.12 g, 3.9 mmol) and potassium carbonate (2.2 g) were refluxed in 50 ml of acetonitrile for 72 h. The crude solid was re-crystallized from methanol (260 mg, 26.1%): m.p. = 177.9°C; ^{1}H-NMR (500 MHz, CDCl$_3$): δ [ppm] = 8.14 (d, 1H, ^3J = 9.8 Hz, 3-H), 7.8 (dd, 4H, ^3J = 5.4 Hz, ^4J = 3.0 Hz, 5-OCH$_2$CH$_2$CH$_2$CH$_2$NC$_8$H$_4$O$_2$), 7.6 (d, 1H, ^3J = 2.4 Hz, 5'-H), 7.13 (s, 1H, 8-H), 6.95 (d, 1H, ^3J = 1.6 Hz, 4'-H), 6.30 (d, 1H, ^3J = 9.8 Hz, 4-H), 4.5 (t, 2H, ^3J = 5.7 Hz, 5-OCH$_2$CH$_2$CH$_2$CH$_2$NC$_8$H$_4$O$_2$), 3.82 (t, 2H, ^3J = 6.6 Hz, 5-OCH$_2$CH$_2$CH$_2$CH$_2$NC$_8$H$_4$O$_2$), 1.98 (p, 4H, ^3J = 3.2 Hz, 5-OCH$_2$CH$_2$CH$_2$CH$_2$NC$_8$H$_4$O$_2$); MS (70 eV) m/z: 403 (13%, M$^+$), 202 (72%, [C$_{11}$H$_6$O$_4$]$^+$), 174 (8%, [202-CO]$^+$), 160 (99%), 148 (6%), 130 (14%), 55 (5%, C$_4$H$_7$); Calculated for C$_{23}$H$_{17}$NO$_6$ (403.40): C, 68.48%; H, 4.25%; N, 3.47%; O, 23.80%. Found: C 68.17%; H, 4.32%; N, 3.36%; LogP: 3.21.

5-(4-Pyrimidynyloxybutoxy)psoralen (PAP-17). 5-(4-Chlorobutoxy)psoralen (500 mg, 1.7 mmol), sodium iodide (512 mg, 3.4 mmol), 4-hydroxypyrimidine (263 mg, 3.4 mmol) and potassium carbonate (3.0 g) were refluxed in 30 ml of acetonitrile for 90 h. The crude product mixture was separated by column chromatography on silica gel (60-200 mesh, 50 g) by gradient elution using a petroleum ether/ethylacetate mixture and yielded PAP-17 and PAP-17a. PAP-17 (99.6 mg, 19.92%, m.p. = 126.4°C) was formed by O-alkylation of 4-hydroxypyrimidine: ^{1}H-NMR (500 MHz, CDCl$_3$): δ [ppm] = 8.80 (s, 1H, 2"-H), 8.47 (d, 1H, ^3J = 9.0 Hz, 6"-H), 8.17 (d, 1H, ^3J = 9.7 Hz, 3-H), 7.60 (d, 1H, ^3J = 2.2 Hz, 5'-H), 7.17 (s, 1H, 8-H), 6.96 (d, 1H, ^3J = 1.8 Hz, 4'-H), 6.74 (d, 1H, ^3J = 5.4 Hz, 5"-H) 6.30 (d, 1H, ^3J = 9.7 Hz, 4-H), 4.54 (t, 2H, ^3J = 5.3 Hz, 5-OCH$_2$CH$_2$CH$_2$CH$_2$OC$_4$H$_3$N$_2$), 4.50 (t, 2H, ^3J = 5.1 Hz, 5-OCH$_2$CH$_2$CH$_2$CH$_2$OC$_4$H$_3$N$_2$), 2.2 (m, 4H, 5-OCH$_2$CH$_2$CH$_2$CH$_2$OC$_4$H$_3$N$_2$); ^{13}C-NMR (DMSO-d_6, 75 MHz): δ [ppm] = 25.38 and 26.68 (5-OCH$_2$(CH$_2$)$_2$CH$_2$OC$_4$H$_3$N$_2$); 65.90 and 72.29 (5-OCH$_2$(CH$_2$)$_2$CH$_2$OC$_4$H$_3$N$_2$); 93.97 (C-8);

105.01 (C-4'); 106.66 (C-4a); 112.61 (C-3 and C-5"); 113.18 (C-6); 139.16 (C-4); 144.84 (C-5');

148.74 (C-5); 152.63 (C-8a); 156.98 (C-6"); 158.20 (C-2") 158.34 (C-7); 161.15 (C-2); 168.83

(C-4"). MS (70 eV) m/z: 352 (24%, M$^+$), 202 (58%, [$C_{11}H_6O_4$]$^+$), 174 (29%, [202-CO]$^+$), 151

(100%, $C_8H_{11}N_2O$), 145 (12%, [174-CO]$^+$), 109 (8%, [$C_6H_5O_2$]$^+$), 97 (60%); Molecular weight

calculated for $C_{19}H_{16}N_2O_5$: 352.10592; Found by high resolution mass spectrometry: 352.10596.

5-[4-(4-Oxopyrimidin-3-yl)butoxy]psoralen (PAP-17a). PAP-17a was formed as a side

product during the synthesis of PAP-17. During the alkylation reaction, 4-hydroxypyrimidine

tautomerises to 4-oxopyrimidine which through N-alkylation formed PAP-17a (248 mg, 49.5%,

m.p = 178.1^{o}C) : ^{1}H-NMR (500 MHz, CDCl$_3$): δ [ppm] = 8.21 (s, 1H, 6"-H), 8.13 (d, 1H, ^3J =

10.1 Hz, 3-H), 7.91 (d, 1H, ^3J = 6.3 Hz, 3"-H), 7.60 (d, 1H, ^3J = 1.7 Hz, 5'-H), 7.17 (s, 1H, 8-H),

6.94 (d, 1H, ^3J = 2.6 Hz, 4'-H), 6.48 (d, ^3J = 6.1 Hz, 4"-H), 6.29 (d, 1H, ^3J = 9.9 Hz, 4-H), 4.49

(t, 2H, ^3J = 6.0 Hz, 5-OC$\underline{H}_2$CH$_2$CH$_2$CH$_2$OC$_4$H$_3$N$_2$), 4.06 (t, 2H, ^3J = 7.35 Hz, 5-

OCH$_2$CH$_2$CH$_2$C$\underline{H}_2$OC$_4$H$_3$N$_2$), 2.2 (m, 4H, 5-OCH$_2$C$\underline{H}_2$C$\underline{H}_2$CH$_2$OC$_4$H$_3$N$_2$); ^{13}C-NMR (DMSO-

d_6, 75 MHz): δ [ppm] = 26.01 and 27.06 (5-O-CH$_2$(C$\underline{H}_2$)$_2$CH$_2$OC$_4$H$_3$N$_2$); 46.92 and 72.01 (5-

OC$\underline{H}_2$(CH$_2$)$_2$C$\underline{H}_2$OC$_4$H$_3$N$_2$); 94.28 (C-8); 104.88 (C-4'); 106.81 (C-4a); 112.87 (C-3); 113.44 (C-

6); 116.16 (C-3"); 139.03 (C-4); 145.03 (C-5'); 148.50 (C-5); 151.02 (C-4"); 152.63 (C-8a);

153.11 (C-6") 158.17 (C-7); 160.82 (C-2"); 161.11 (C-2). MS (70 eV) m/z: 352 (13%, M$^+$), 202

(12%, [$C_{11}H_6O_4$]$^+$), 174 (10%, [202-CO]$^+$), 151 (100%, $C_8H_{11}N_2O$), 145 (5%, [174-CO]$^+$), 109

(6%, [$C_6H_5O_2$]$^+$), 97 (27%); Molecular weight calculated for $C_{19}H_{16}N_2O_5$: 352.1059; Found by

high resolution mass spectrometry: 352.1066.

5-(4-Phenoxybutoxy)psoralen (PAP-1). 5-HOP (700 mg, 3.5 mmol), 4-phenoxybutyl bromide

(600 mg, 3.5 mmol) and potassium carbonate (2.0 g) were refluxed in 30 ml of 2-butanone for 24

h. The crude product was re-crystallized from methanol-acetone (80:20) as a white solid (734

mg, 60.5%): m.p. = 104°C; ^{1}H-NMR (500 MHz, CDCl$_3$): δ [ppm] = 8.13 (d, 1H, ^3J = 9.7 Hz, 3-H), 7.59 (d, 1H, ^3J = 2.0 Hz, 5'-H), 7.30 (m, 5H, 5-OCH$_2$CH$_2$CH$_2$CH$_2$OC$_6$H$_5$), 7.15 (s, 1H, 8-H), 6.91 (d, 1H, ^3J = 2.0 Hz, 4'-H), 6.25 (d, 1H, ^3J = 9.8 Hz, 4-H), 4.56 (t, 2H, ^3J = 6.14 Hz, 5-OCH$_2$CH$_2$CH$_2$CH$_2$OC$_6$H$_5$), 4.09 (t, 2H, ^3J = 5.80 Hz, 5-OCH$_2$CH$_2$CH$_2$CH$_2$OC$_6$H$_5$), 2.09 (m, 4H, ^3J = 4.21 Hz, 5-OCH$_2$CH$_2$CH$_2$CH$_2$OC$_6$H$_5$); ^{13}C-NMR (DMSO-d_6, 75 MHz): δ [ppm] = 25.26 and 26.18 (5-O-CH$_2$(CH$_2$)$_2$CH$_2$OC$_6$H$_5$); 66.91 and 72.29 (5-OCH$_2$(CH$_2$)$_2$CH$_2$OC$_6$H$_5$); 93.18 (C-8); 105.62 (C-4'); 105.98 (C-4a); 112.29 (C-3); 112.92 (C-6); 114.39 (C-3" and C-5"); 120.39 (C-4"); 129.41 (C-2" and C-6"); 139.44 (C-4); 145.89 (C-5'); 148.72 (C-5); 152.11 (C-8a); 157.63 (C-1"); 158.48 (C-7); 160.07 (C-2); MS (70 eV) m/z: 350 (20%, M$^+$), 202 (9%, [C$_{11}$H$_6$O$_4$]$^+$), 201 (5%), 174 (13%, [202-CO]$^+$), 173 (4%), 150 (11%), 149 (100%), 145 (8%), 107 (100%, [149-C$_3$H$_6$]$^+$), 94 (9%, C$_6$H$_6$O), 89 (4%), 77 (37%, C$_6$H$_5$), 65 (6%, C$_5$H$_5$); Calculated for C$_{21}$H$_{18}$O$_5$ (350.37): C, 71.99%; H, 5.18%; O, 22.83%. Found: C,71.92%; H, 5.08%; LogP: 4.06.

5-(3-Phenoxypropoxy)psoralen (PAP-3). 5-HOP (700 mg, 3.5 mmol), 3-phenoxypropyl bromide (750 mg, 3.5 mmol) and potassium carbonate (3.0 g) were refluxed in 30 ml of 2-butanone for 36 h. The oily residue was re-crystallized from methanol/ethyl acetate (10:90) as a white solid (390 mg, 33.5%): m.p. = 108.4°C; ^{1}H-NMR (500 MHz, CDCl$_3$): δ [ppm] = 8.13 (d, 1H, ^3J = 9.8 Hz, 3-H), 7.59 (d, 1H, ^3J = 2.3 Hz, 5'-H), 7.31 (t, 3H, 3"-H, 4"-H, 5"-H), 7.16 (s, 1H, 8-H), 6.99 (d, 1H, ^3J = 2.4 Hz, 4'-H), 6.93 (d, 2H, 2"-H, 6"-H), 6.24 (d, 1H, ^3J = 9.5 Hz, 4-H), 4.66 (t, 2H, ^3J = 5.9 Hz, 5-OCH$_2$CH$_2$CH$_2$OC$_6$H$_5$), 4.26 (t, 2H, ^3J = 6.0 Hz, 5-OCH$_2$CH$_2$CH$_2$OC$_6$H$_5$), 2.38 (p, 2H, ^3J = 6.0 Hz, 5-OCH$_2$CH$_2$CH$_2$OC$_6$H$_5$); MS (70 eV) m/z: 336 (91%, M$^+$), 203 (7%), 202 (57%, [C$_{11}$H$_6$O$_4$]$^+$), 201 (11%), 174 (16%, [202-CO]$^+$), 173 (11%), 145 (14%), 135 (90%), 134 (9%), 108 (8%), 107 (100%), 95 (8%), 89 (9%), 77 (62%, C$_6$H$_5$), 65

(9%, C_5H_5); Calculated for $C_{21}H_{18}O_5$ (336.35): C, 71.42%; H, 4.79%; O, 23.78%. Found: C, 71.09%, H, 4.74%. LogP: 3.76.

5-(2-Benzyloxyethoxy)psoralen (PAP-5). 5-HOP (600 mg, 2.9 mmol), benzyl-2-bromoethyl ether (1.0 g, 4.6 mmol) and potassium carbonate (2.0 g) were refluxed in 30 ml of 2-butanone for 16 h. The oily residue was re-crystallized from 70% methanol to obtain a white solid (123 mg, 12.3%): m.p. = 90.9°C; ^{1}H-NMR (500 MHz, CDCl$_3$): δ [ppm] = 8.19 (d, 1H, ^3J = 9.7 Hz, 3-H), 7.59 (d, 1H, ^3J = 2.2 Hz, 5'-H), 7.37 (m, 5H, 5-OCH$_2$CH$_2$OCH$_2$C$_6$<u>H</u>$_5$), 7.19 (s, 1H, 8-H), 6.95 (d, 1H, ^3J = 2.0 Hz, 4'-H), 6.25 (d, 1H, ^3J = 9.7 Hz, 4-H), 4.64 (s, 2H, 5-OCH$_2$CH$_2$OC<u>H</u>$_2$C$_6$H$_5$), 4.58 (t, 2H, ^3J = 4.62 Hz, 5-OC<u>H</u>$_2$CH$_2$OCH$_2$C$_6$H$_5$), 3.88 (t, 2H, ^3J = 4.56 Hz, 5-OCH$_2$C<u>H</u>$_2$OCH$_2$C$_6$H$_5$); MS (70 eV) m/z: 336 (35%, M$^+$), 105 (5%), 91 (100%, [C$_7$H$_7$]$^+$); Calculated for $C_{20}H_{16}O_5$ (336.35): C, 71.42%; H, 4.79%; O, 23.78%. Found: C, 70.65%; H, 4.73%; LogP: 3.34.

5-(5-Phenoxypentoxy)psoralen (AS-121). 1-Bromo-5-phenoxypentane was synthesized according to General Method C using 1,5-dibromopentane instead of 1,4-dibromobutane. 5-HOP (300 mg, 1.5 mmol), 1-bromo-5-phenoxypentane (600 mg, 2.6 mmol) and potassium carbonate (2.0 g) were then refluxed in 30 ml of acetone for 24 h. The crude product was re-crystallized from methanol/water (80:20) as a white solid (232 mg, 42.4%): m.p. = 91 °C; ^{1}H-NMR (300 MHz, DMSO-d_6): δ [ppm] = 8.19 (d, 1H, ^3J = 9.7 Hz, 4-H), 8.02 (s, 1H, 5'-H), 7.25-7.33 (m, 4H, 8-H, 4'-H and 5-OCH$_2$CH$_2$CH$_2$CH$_2$CH$_2$OC$_6$<u>H</u>$_5$), 6.90-6.93 (m, 3H, 5-OCH$_2$CH$_2$CH$_2$CH$_2$CH$_2$OC$_6$<u>H</u>$_5$), 6.30 (d, 1H, ^3J = 9.7 Hz, 3-H), 4.52 (t, 2H, ^3J = 6.0 Hz, 5-OC<u>H</u>$_2$CH$_2$CH$_2$CH$_2$CH$_2$OC$_6$H$_5$), 4.00 (t, 2H, ^3J = 6.2 Hz, 5-OCH$_2$CH$_2$CH$_2$CH$_2$C<u>H</u>$_2$OC$_6$H$_5$), 1.77-1.93 (m, 4H, 5-OCH$_2$C<u>H</u>$_2$CH$_2$C<u>H</u>$_2$CH$_2$OC$_6$H$_5$), 1.63-1.71 (m, 2H, 5-OCH$_2$CH$_2$C<u>H</u>$_2$CH$_2$CH$_2$OC$_6$H$_5$); MS (70 eV) m/z: 364 M$^+$ (9%, M$^+$), 202 (22%, [C$_{11}$H$_6$O$_4$]$^+$), 163

(44%, $[C_{11}H_{15}O]^+$), 107 (40%, $[C_6H_5O\text{-}CH_2]^+$), 69 (100%, $[C_5H_9]^+$), 41 (52%, $[C_3H_5]^+$); Calculated for $C_{22}H_{20}O_5$ (364.40): C, 72.51%; H, 5.53%; O, 21.96%. Found: C, 72.74%; H, 5.68%; LogP: 4.40.

5-(4-Benzyloxybutoxy)psoralen (PAP-6). 5-HOP (700 mg, 3.5 mmol), benzyl-4-bromobutyl ether (850 mg, 3.5 mmol) and potassium carbonate (2.0 g) were refluxed in 30 ml of 2-butanone for 24 h. The oily residue was re-crystallized from 80% methanol (171 mg, 13.4%): m.p. = 78.4°C; ^{1}H-NMR (500 MHz, CDCl$_3$): δ [ppm] = 8.14 (d, 1H, ^3J = 9.8 Hz, 3-H), 7.55 (d, 1H, ^3J = 2.5 Hz, 5'-H), 7.34 (m, 5H, 5-OCH$_2$CH$_2$CH$_2$CH$_2$OCH$_2$C$_6$<u>H</u>$_5$), 7.13 (s, 1H, 8-H), 6.91 (d, 1H, ^3J = 2.4 Hz, 4'-H), 6.25 (d, 1H, ^3J = 9.8 Hz, 4-H), 4.54 (s, 2H, 5-OCH$_2$CH$_2$CH$_2$CH$_2$OC<u>H</u>$_2$C$_6$H$_5$), 4.49 (t, 2H, ^3J = 6.5 Hz, 5-OC<u>H</u>$_2$CH$_2$CH$_2$CH$_2$OCH$_2$C$_6$H$_5$), 3.59 (t, 2H, ^3J = 6.1 Hz, 5-OCH$_2$CH$_2$CH$_2$C<u>H</u>$_2$OCH$_2$C$_6$H$_5$), 2.00 (p, 2H, ^3J = 6.9 Hz, 5-OCH$_2$C<u>H</u>$_2$CH$_2$CH$_2$OCH$_2$C$_6$H$_5$), 1.87 (p, 2H, ^3J = 6.8 Hz, 5-OCH$_2$CH$_2$C<u>H</u>$_2$CH$_2$OCH$_2$C$_6$H$_5$); MS (70 eV) m/z: 364 (37%, M$^+$), 292 (10%), 202 (7%, $[C_{11}H_6O_4]^+$), 174 (6%, $[202\text{-}CO]^+$), 163 (12%), 91 (100%, C$_7$H$_7$), 71 (8%); Calculated for $C_{22}H_{20}O_5$ (364.40): C, 72.51%; H, 5.53%; O, 21.95%. Found: C, 72.36%; H, 5.46%; LogP: 4.02.

5-(3-Benzyloxypropoxy)psoralen (PAP-7). 5-HOP (1.0 g, 4.9 mmol), benzyl-3-bromopropyl ether (1.36 g, 5.9 mmol) and potassium carbonate (3.4 g) were refluxed in 30 ml of 2-butanone for 24 h. The oily residue was re-crystallized from 70% methanol (700 mg, 40.4%): m.p. = 75.2°C; ^{1}H-NMR (500 MHz, CDCl$_3$): δ [ppm] = 8.06 (d, 1H, ^3J = 9.7 Hz, 3-H), 7.57 (d, 1H, ^3J = 2.2 Hz, 5'-H), 7.29 (m, 5H, ^3J = 6.3 Hz, 5-OCH$_2$CH$_2$CH$_2$OCH$_2$C$_6$<u>H</u>$_5$), 7.15 (s, 1H, 8-H), 6.98 (d, 1H, ^3J = 2.2 Hz, 4'-H), 6.21 (d, 1H, ^3J = 9.8 Hz, 4-H), 4.58 (t, 2H, ^3J = 6.1 Hz, 5-OC<u>H</u>$_2$CH$_2$CH$_2$OCH$_2$C$_6$H$_5$), 4.55 (s, 2H, 5-OCH$_2$CH$_2$CH$_2$OC<u>H</u>$_2$C$_6$H$_5$), 3.73 (t, 2H, ^3J = 5.7 Hz, 5-OCH$_2$CH$_2$C<u>H</u>$_2$OCH$_2$C$_6$H$_5$), 2.18 (p, 2H, ^3J = 6.1 Hz, 5-OCH$_2$C<u>H</u>$_2$CH$_2$OCH$_2$C$_6$H$_5$); MS (70 eV)

m/z: 350 (25%, M$^+$), 202 (9%, [C$_{11}$H$_6$O$_4$]$^+$), 174 (5%, [202-CO]$^+$), 91 (100%, [C$_7$H$_7$]$^+$); Calculated for C$_{21}$H$_{18}$O$_5$(350.37): C, 71.99%; H, 5.18%; O, 22.83%. Found: C, 71.64%; H, 5.34%; LogP: 3.66.

5-(4-Phenyl-3-oxobutoxy)psoralen (KP-1). 4-Chlorobutyrophenone (497 mg, 2.7 mmol) and sodium iodide (445 mg, 2.9 mmol) were refluxed in 30 ml acetone for 1.5 h to obtain the iodo derivative. To this slurry were added 5-HOP (500 mg, 2.5 mmol), potassium carbonate (2.0 g) and the resulting mixture then refluxed for 140 h. The solid residue was re-crystallized from a petroleum ether/acetone (90:10) mixture (295 mg, 34.3%): m.p = 129.1^{o}C; ^{1}H-NMR (500 MHz, CDCl$_3$): δ [ppm] = 8.13 (d, 1H, ^3J = 9.9 Hz, 3-H), 8.01 (d, 2H, ^3J = 7.9 Hz, ^4J = 0.95 Hz, 2"-H, 6"-H), 7.62 (t, 1H, ^3J = 7.4 Hz, 3"-H, 5"-H), 7.60 (d, 1H, ^3J = 2.4 Hz, 5'-H), 7.50 (t, 2H, ^3J = 7.7 Hz, 4"-H), 7.15 (s, 1H, 8-H), 6.99 (d, 1H, ^3J = 2.5 Hz, 4'-H), 6.26 (d, 1H, ^3J = 9.8 Hz, 4-H) 4.59 (t, 2H, ^3J = 6.2 Hz, 5-OCH$_2$CH$_2$CH$_2$COC$_6$H$_5$), 3.28 (t, 2H, ^3J = 6.8 Hz, 5-OCH$_2$CH$_2$CH$_2$COC$_6$H$_5$), 2.38 (p, 2H, ^3J = 6.5 Hz, 5-OCH$_2$CH$_2$CH$_2$COC$_6$H$_5$); MS (70 eV) m/z: 348 (34%, M$^+$), 202 (5%, [C$_{11}$H$_6$O$_4$]$^+$), 147(99%, C$_{10}$H$_{10}$O), 174, (5%, [202-CO]$^+$), 105 (71%, C$_3$H$_6$), 77 (33%, C$_6$H$_5$); Calculated for C$_{21}$H$_{16}$O$_5$ (348.36): C, 72.41%; H, 4.63%; O, 22.96%. Found: C, 72.18%; H, 4.75%; LogP: 3.31.

5-[4-(4-Methoxyphenoxy)butoxy]psoralen (AS-67). 5-HOP (300 mg, 1.5 mmol), 1-bromo-4-(4-methoxyphenoxy)butane (600 mg, 2.5 mmol, obtained by General Method C) and potassium carbonate (2.0 g) were refluxed in 30 ml of acetone for 24 h. The crude product was re-crystallized from methanol-water (80:20) as a white solid (201 mg, 35.2%): m.p. = 111.5 °C; ^{1}H-NMR (300 MHz, DMSO-d_6): δ [ppm] = 8.18 (d, 1H, ^3J = 9.8 Hz, 4-H), 8.03 (d, 1H, ^3J = 2.3 Hz, 5'-H), 7.32-7.34 (m, 2H, 8-H and 4'-H), 6.81-6.87 (m, 4H, 5-OCH$_2$(CH$_2$)$_2$CH$_2$OC$_6$H$_4$OCH$_3$), 6.81-6.87 (m, 4H, 5-OCH$_2$(CH$_2$)$_2$CH$_2$OC$_6$H$_4$OCH$_3$), 6.30 (d, 1H, ^3J = 9.8 Hz, 3-H), 4.57 (t, 2H, ^3J = 5.7 Hz, 5-

OC$\underline{H}_2$(CH$_2$)$_2$CH$_2$OC$_6$H$_4$OCH$_3$), 4.00 (t, 2H, ^3J = 5.8 Hz, 5-OCH$_2$(CH$_2$)$_2$C$\underline{H}_2$OC$_6$H$_4$OCH$_3$), 3.69 (s,

3H, -OC$\underline{H}_3$), 1.91-1.99 (m, 4H, 5-OCH$_2$(C$\underline{H}_2$)$_2$CH$_2$OC$_6$H$_4$OCH$_3$); MS (70 eV) m/z: 380 (14%,

M$^+$), 257 (8%), 215 (7%), 202 (5%, [C$_{11}$H$_6$O$_4$]$^+$), 179 (69%, [C$_{11}$H$_{15}$O$_2$]$^+$), 145 (6%), 137 (100%,

[CH$_3$OC$_6$H$_4$OCH$_2$]$^+$), 109 (29%), 107 (18%, [C$_6$H$_5$OCH$_2$]$^+$), 77 (23%, [C$_6$H$_5$]$^+$), 55 (61%,

[C$_4$H$_7$]$^+$), 41 (15%, [C$_3$H$_5$]$^+$); Calculated for C$_{22}$H$_{20}$O$_6$ (380.4): C, 69.46%; H, 5.30%; O, 25.24%.

Found: C, 69.52%; H, 5.39%; Log P: 3.89.

5-[4-(3-Methoxyphenoxy)butoxy]psoralen (AS-68). 5-HOP (300 mg, 1.5 mmol), 1-bromo-4-

(3-methoxyphenoxy)butane (600 mg, 2.5 mmol, obtained by general method C) and potassium

carbonate (2.0 g) were refluxed in 30 ml of acetone for 24 h. The crude product was re-

crystallized from methanol-water (80:20) as a white solid (178 mg, 31.2%): m.p. = 102.5 °C; ^{1}H-

NMR (300 MHz, DMSO-d_6): δ [ppm] = 8.18 (d, 1H, ^3J = 9.8 Hz, 4-H), 8.02 (d, 1H, ^3J = 1.9 Hz,

5"-H), 7.33 (s, 2H, 8-H and 4'-H), 7.15 (t, 1H, ^3J = 8.14 Hz, 8-H), 6.45-6.51 (m, 3H, 2"-H, 4"-H

and 6"-H), 6.29 (d, 1H, ^3J = 9.8 Hz, 3-H), 4.58 (t, 2H, ^3J = 5.4 Hz, 5-

OC$\underline{H}_2$(CH$_2$)$_2$CH$_2$OC$_6$H$_4$OCH$_3$), 4.05 (t, 2H, ^3J = 5.4 Hz, 5-O-CH$_2$(CH$_2$)$_2$C$\underline{H}_2$OC$_6$H$_4$OCH$_3$), 3.71

(s, 3H, -OC$\underline{H}_3$), 1.91-1.99 (m, 4H, 5-OCH$_2$(C$\underline{H}_2$)$_2$CH$_2$OC$_6$H$_4$OCH$_3$); MS (70 eV) m/z : 380

(14%, M$^+$), 257 (8%), 202 (5%, [C$_{11}$H$_6$O$_4$]$^+$), 179 (84%, [C$_{11}$H$_{15}$O$_2$]$^+$), 145 (6%), 137 (100%,

[CH$_3$OC$_6$H$_4$OCH$_2$]$^+$), 109 (14%), 107 (32%, [C$_6$H$_5$OCH$_2$]$^+$), 77 (27%, [C$_6$H$_5$]$^+$), 55 (63%,

[C$_4$H$_7$]$^+$), 41 (12%, [C$_3$H$_5$]$^+$); Calculated for C$_{22}$H$_{20}$O$_6$ (380.4): C, 69.46%; H, 5.30; O, 25.24%.

Found: C, 69.89%; H, 5.38%; LogP: 3.99.

5-[4-(3,5-Dimethoxyphenoxy)butoxy]psoralen (AS-69). 5-HOP (300 mg, 1.5 mmol), 1-

bromo-4-(3,5-dimethoxyphenoxy)butane (700 mg, 2.6 mmol, obtained by General Method C)

and potassium carbonate (2.0 g) were refluxed in 30 ml of acetone for 24 h. The crude product

was re-crystallized from methanol/acetone (80:20) as a white solid (182 mg, 29.6%): m.p. = 139

°C; ^{1}H-NMR (300 MHz, DMSO-d_6): δ [ppm] = 8.19 (d, 1H, ^3J = 9.8 Hz, 4-H), 8.03 (d, 1H, ^3J = 2.1 Hz, 5'-H), 7.34 (s, 2H, 8-H and 4'-H), 6.31 (d, 1H, ^3J = 9.8 Hz, 3-H), 6.07 (s, 3H, 2"-H, 4"-H and 6"-H), 4.58 (t, 2H, ^3J = 5.4 Hz, 5-OC$\underline{H}_2$(CH$_2$)$_2$CH$_2$OC$_6$H$_3$(OCH$_3$)$_2$), 4.05 (t, 2H, ^3J = 5.4 Hz, 5-OCH$_2$(CH$_2$)$_2$C$\underline{H}_2$OC$_6$H$_3$(OCH$_3$)$_2$), 3.69 (s, 6H, -(OC$\underline{H}_3$)$_2$), 1.93-1.97 (m, 4H, 5-OCH$_2$(C$\underline{H}_2$)$_2$CH$_2$OC$_6$H$_3$(OCH$_3$)$_2$); MS (70 eV) m/z: 410 (12%, M$^+$), 209 (100%, [C$_{12}$H$_{17}$O$_3$]$^+$), 202 (5%, [C$_{11}$H$_6$O$_4$]$^+$), 167 (75%, [(CH$_3$O)$_2$C$_6$H$_3$OCH$_2$]$^+$), 137 (34%, [CH$_3$OC$_6$H$_4$OCH$_2$]$^+$), 122 (15%), 107 (10%, [C$_6$H$_5$OCH$_2$]$^+$), 77 (11%, [C$_6$H$_5$]$^+$), 55 (46%, [C$_4$H$_7$]$^+$), 41 (6%, [C$_3$H$_5$]$^+$); Calculated for C$_{23}$H$_{22}$O$_7$ (410.43): C, 67.31%; H, 5.40%; O, 27.29%. Found: C, 66.92%; H, 5.60%; LogP: 3.94.

5-[4-(4-Nitrophenoxy)butoxy]psoralen (AS-78). 5-HOP (300 mg, 1.5 mmol), 1-bromo-4-(4-nitrophenoxy)butane (700 mg, 2.7 mmol, obtained by General Method C) and potassium carbonate (2.0 g) were refluxed in 30 ml of acetone for 24 hours. The crude product was re-crystallized from methanol/acetone (80:20) as a yellow solid (291 mg, 49.1%): m.p. = 132°C; ^{1}H-NMR (300 MHz , DMSO-d_6): δ [ppm] = 8.16 (d, 2H, ^3J = 9.1 Hz, 3"-H and 5"-H), 8.15 (d, 1H, ^3J = 9.6 Hz, 4-H), 8.00 (d, 1H, ^3J = 2.1 Hz, 5'-H), 7.30 (d, 1H, ^3J = 1.9 Hz, 4'-H), 7.28 (s, 1H, 8-H), 7.10 (d, 2H, ^3J = 9.2 Hz, 2"-H and 6"-H), 6.27 (d, 1H, ^3J = 9.8 Hz, 3-H), 4.56 (s, 2H, 5-OC$\underline{H}_2$(CH$_2$)$_2$CH$_2$OC$_6$H$_4$NO$_2$), 4.05 (s, 2H, 5-OCH$_2$(CH$_2$)$_2$C$\underline{H}_2$OC$_6$H$_4$NO$_2$), 1.99 (s, 4H, 5-OCH$_2$(C$\underline{H}_2$)$_2$CH$_2$OC$_6$H$_4$NO$_2$); MS (70 eV) m/z: 395 (12%, M$^+$), 202 (30%, [C$_{11}$H$_6$O$_4$]$^+$), 194 (100%, [C$_{10}$H$_{12}$O$_3$N]$^+$), 174 (26%, [202-CO]$^+$), 152 (82%, [O$_2$NC$_6$H$_4$OCH$_2$]$^+$), 133 (17%), 106 (17%), 89 (13%), 75 (12%), 55 (84%, [C$_4$H$_7$]$^+$), 41 (11%); Calculated for C$_{21}$H$_{17}$O$_7$ (395.34): C, 63.80%; H, 4.33%; N, 3.54%; O, 28.33%. Found: C, 63.79%; H, 4.46%; N, 3.60%; Log P: 3.91.

5-[4-(4-Chlorphenoxy)butoxy]psoralen (AS-84). 5-HOP (300 mg, 1.5 mmol), 1-bromo-4-(4-chlorophenoxy)butane (700 mg, 2.8 mmol, obtained by General Method C) and potassium

carbonate (2.0 g) were refluxed in 30 ml of acetone for 24 hours. The crude product was re-crystallized from methanol/water (80:20) as a white solid (247 mg, 42.8%): m.p. = 142.5°C; ^{1}H-NMR (300 MHz, DMSO-d_6): δ [ppm] = 8.15 (d, 1H, ^3J = 9.8 Hz, 4-H), 8.01 (d, 1H, ^3J = 2.0 Hz, 5'-H), 7.31 (s, 2H, 8-H and 4'-H), 7.29 (d, 2H, ^3J = 8.9 Hz, 3"-H and 5"-H), 6.93 (d, 2H, ^3J = 8.9 Hz, 2"-H and 6"-H), 6.28 (d, 1H, ^3J = 9.8 Hz, 3-H), 4.55 (m, 2H, 5-OC$\underline{H}_2$(CH$_2$)$_2$CH$_2$OC$_6$H$_4$Cl), 4.05 (m, 2H, 5-OCH$_2$(CH$_2$)$_2$C$\underline{H}_2$OC$_6$H$_4$Cl), 1.95-1.96 (m, 4H, 5-OCH$_2$(C$\underline{H}_2$)$_2$CH$_2$OC$_6$H$_4$Cl); MS (70 eV) m/z: 384 (10%, M$^+$), 202 (14%, [C$_{11}$H$_6$O$_4$]$^+$), 183 (80%, [C$_{10}$H$_{12}$OCl]$^+$), 174 (11%, [202-CO]$^+$), 141 (100%, [ClC$_6$H$_4$OCH$_2$]$^+$), 113 (18%), 111 (23%), 89 (7%), 77 (9%, [C$_6$H$_5$]$^+$), 55 (72%, [C$_4$H$_7$]$^+$), 41 (5%); Calculated for C$_{21}$H$_{17}$ClO$_5$ (384.82): C, 65.55%; H, 4.45%; Cl, 9.21%; O, 20.79%. Found: C, 65.23%; H, 4.57%; LogP: 4.50.

5-[4-(4-Phenoxyphenoxy)butoxy]psoralen (AS-85). 5-HOP (300 mg, 1.5 mmol), 1-bromo-4-(4-phenoxyphenoxy)butane (800 mg, 2.5 mmol, obtained by General Method C) and potassium carbonate (2.0 g) were refluxed in 30 ml of acetone for 24 h. The crude product was re-crystallized from ethanol/acetone (70:30) as a white solid (165 mg, 24.9%): m.p. = 137°C; ^{1}H-NMR (300 MHz, DMSO-d_6): δ [ppm] = 8.17 (d, 1H, ^3J = 9.8 Hz, 4-H), 8.02 (s, 1H, 5'-H), 7.31-7.35 (m, 4H, 8-H, 4'-H and -O-C$_6$$\underline{H}_4OC_6$$\underline{H}_5$), 7.06 (t, 1H, 4'''-H), 6.89-6.96 (m, 6H, -OC$_6$$\underline{H}_4OC_6$$\underline{H}_5$), 6.29 (d, 1H, ^3J = 9.7 Hz, 3-H), 4.57 (s, 2H, 5-OC$\underline{H}_2$(CH$_2$)$_2$CH$_2$OC$_6$H$_4$OC$_6$H$_5$), 4.05 (s, 2H, 5-OCH$_2$(CH$_2$)$_2$C$\underline{H}_2$OC$_6$H$_4$OC$_6$H$_5$), 1.97 (s, 4H, 5-OCH$_2$(C$\underline{H}_2$)$_2$CH$_2$OC$_6$H$_4$OC$_6$H$_5$); MS (70 eV) m/z: 442 (25%, M$^+$), 257 (16%), 241 (100%, [C$_6$H$_5$OC$_{10}$H$_{12}$O]$^+$), 215 (12%), 199 (100%, [C$_6$H$_5$OC$_8$H$_8$O]$^+$), 186 (100%, [C$_6$H$_5$OC$_7$H$_5$O]$^+$), 171 (12%), 148 (38%), 129 (13%), 115 (17%), 93 (10%), 77 (49%, [C$_6$H$_5$]$^+$), 55 (70%, [C$_4$H$_7$]$^+$), 41 (7%); Calculated for C$_{27}$H$_{22}$O$_6$ (442.47): C, 73.29%; H, 5.01%; O, 21.7%. Found: C, 73.24%; H, 5.09%; LogP: 5.03.

5-[4-(4-Methylphenoxy)butoxy]psoralen (AS-96). 5-HOP (300 mg, 1.5 mmol), 1-bromo-4-(4-

methylphenoxy)butane (600 mg, 2.5 mmol, obtained by General Method C) and potassium carbonate (2.0 g) were refluxed in 30 ml of acetone for 24 h. The crude product was re-crystallized from methanol/acetone (80:20) as a white solid (253 mg, 46.3%): m.p. = 128°C; ^{1}H-NMR (300 MHz, DMSO-d_6): δ [ppm] = 8.15 (d, 1H, ^3J = 9.8 Hz, 4-H), 8.02 (d, 1H, ^3J = 2.1 Hz, 5'-H), 7.31 (s, 2H, 8-H and 4'-H), 7.06 (d, 2H, ^3J = 8.4 Hz, 2"-H and 6"-H), 6.80 (d, 2H, ^3J = 8.5 Hz, 3"-H and 5"-H), 6.28 (d, 1H, ^3J = 9.8 Hz, 3-H), 4.56 (t, 2H, ^3J = 5.6 Hz, 5-OC$\underline{H}_2$(CH$_2$)$_2$CH$_2$OC$_6$H$_4$CH$_3$), 4.02 (t, 2H, ^3J = 5.7 Hz, 5-OCH$_2$(CH$_2$)$_2$C$\underline{H}_2$OC$_6$H$_4$CH$_3$), 2.22 (s, 3H, -CH$_3$), 1.92-2.01 (m, 4H, 5-OCH$_2$(C$\underline{H}_2$)$_2$CH$_2$OC$_6$H$_4$CH$_3$); MS (70 eV) m/z: 364 (10%, M$^+$), 202 (5%, [C$_{11}$H$_6$O$_4$]$^+$), 163 (87%, [C$_{11}$H$_{15}$O]$^+$), 121 (100%, [CH$_3$C$_6$H$_4$OCH$_2$]$^+$), 91 (33%, [C$_7$H$_7$]$^+$), 65 (9%), 55 (35%, [C$_4$H$_7$]$^+$), 41 (4%); Calculated for C$_{22}$H$_{20}$O$_5$ (364.40): C, 72.51%; H, 5.53%; O, 21.96%. Found: C, 72.59%; H, 5.65%; LogP: 4.42.

5-[4-(4-Fluorphenoxy)butoxy]psoralen (AS-111). 5-HOP (300 mg, 1.5 mmol), 1-bromo-4-(4-fluorophenoxy)butane (600 mg, 2.5 mmol, obtained by General Method C) and potassium carbonate (2.0 g) were refluxed in 30 ml of acetone for 24 h. The crude product was re-crystallized from methanol/water (80:20) as a white solid (192 mg, 34.7%): m.p. = 121°C; ^{1}H-NMR (300 MHz, DMSO-d_6): δ [ppm] = 8.14 (d, 1H, ^3J = 9.8 Hz, 4-H), 8.01 (d, 1H, ^3J = 2.0 Hz, 5'-H), 7.30 (s, 2H, 4'-H and 8-H), 6.89-6.94 (m, 2H, 5-OCH$_2$(CH$_2$)$_2$CH$_2$OC$_6$$\underline{H}_4$F), 6.27 (d, 1H, ^3J = 9.8 Hz, 3-H), 4.53-4.55 (m, 2H, 5-OC$\underline{H}_2$(CH$_2$)$_2$CH$_2$OC$_6$H$_4$F), 4.01-4.05 (m, 2H, 5-OCH$_2$(CH$_2$)$_2$C$\underline{H}_2$OC$_6$H$_4$F), 1.94-1.96 (m, 4H, 5-OCH$_2$(C$\underline{H}_2$)$_2$CH$_2$OC$_6$H$_4$F); MS (70 eV) m/z: 368 (11%, M$^+$), 202 (11%, [C$_{11}$H$_6$O$_4$]$^+$), 174 (11%, [202-CO]$^+$), 167 (83%, [C$_{10}$H$_{12}$OF]$^+$), 125 (100%, [FC$_6$H$_4$OCH$_2$]$^+$), 95 (23%), 89 (5%), 55 (46%, [C$_4$H$_7$]$^+$), 41 (3%); Calculated for C$_{21}$H$_{17}$FO$_5$ (368.37): C, 68.47%; H, 4.65%; F, 5.16%; O, 21.72%. Found: C, 68.15%; H, 4.65; LogP: 4.11.

5-[4-(3-Trifluormethylphenoxy)butoxy]psoralen (AS-118). 5-HOP (300 mg, 1.5 mmol), 1-

bromo-4-(3-trifluoromethylphenoxy)butane (700 mg, 2.4 mmol, obtained by General Method C) and potassium carbonate (2.0 g) were refluxed in 30 ml of acetone for 24 hours. The crude product was re-crystallized from methanol/acetone (60:40) as a white solid (142 mg, 22.6%): m.p. = 118°C; ^{1}H-NMR (300 MHz, DMSO-d_6): δ [ppm] = 8.15 (d, 1H, ^3J = 9.8 Hz, 4-H), 8.01 (d, 1H, ^3J = 2.3 Hz, 5'-H), 7.49 (t, 1H, ^3J = 7.93 Hz, 5"-H), 7.18-7.32 (m, 5H, 2"-H, 4"-H, 6"-H, 8-H and 4'-H), 6.26 (d, 1H, ^3J = 9.8 Hz, 3-H), 4.57 (s, 2H, 5-OC$\underline{H}_2$(CH$_2$)$_2$CH$_2$OC$_6$H$_4$CF$_3$), 4.15 (s, 2H, 5-O-CH$_2$(CH$_2$)$_2$C$\underline{H}_2$OC$_6$H$_4$CF$_3$), 1.98 (s, 4H, 5-OCH$_2$(C$\underline{H}_2$)$_2$CH$_2$OC$_6$H$_4$CF$_3$); MS (70 eV) m/z: 418 (14%, M$^+$), 217 (79%), 202 (19%, [C$_{11}$H$_6$O$_4$]$^+$), 175 (100%, [C$_{12}$H$_{15}$O]$^+$), 145 (37%), 127 (7%), 109 (14%), 89 (6%), 55 (75%, [C$_4$H$_7$]$^+$), 41 (4%); Calculated for C$_{22}$H$_{17}$F$_3$O$_5$ (418.37): C, 63.16%; H, 4.10%; F, 13.62%; O, 19.12%. Found: C, 63.19%; H, 4.09%; LogP: 4.65.

5-(4-[2Methoxy-4-nitrophenoxy]butoxy)psoralen (PAP-10). 5-(4-Chlorobutoxy)psoralen (500 mg, 1.7 mmol) and sodium iodide (741 mg, 4.9 mmol) were refluxed in 15 ml of anhydrous acetonitrile for 60 min to obtain the iodo derivative. To this solution were added 4-nitroguaicol (837 mg, 4.9 mmol), potassium carbonate (3.0 g) and 10 ml of acetonitrile and the mixture refluxed for 72 h. The solid residue was re-crystallized from a methanol/acetone (80:20) mixture (382 mg, 52.6%): m.p. = 170.5°C; ^{1}H-NMR (500 MHz, CDCl$_3$): δ [ppm] = 8.15 (d, 1H, ^3J = 9.8 Hz, 3-H), 7.91 (d, 1H, ^4J = 2.6 Hz, 3"-H), 7.75 (dd, 1H, ^3J = 2.7 Hz, 5"-H), 7.60 (d, 1H, ^3J = 2.2 Hz, 5'-H), 7.16 (s, 1H, 8-H), 6.98 (d, 1H, ^3J = 2.4 Hz, 4'-H), 6.93 (d, 1H, ^3J = 2.2 Hz, 6"-H), 6.26 (d, 1H, ^3J = 9.7 Hz, 4-H), 4.59 (t, 2H, ^3J = 6.0 Hz, 5-OC$\underline{H}_2$CH$_2$CH$_2$CH$_2$OC$_6$H$_3$), 4.23 (t, 2H, ^3J = 5.7 Hz, 5-OCH$_2$CH$_2$CH$_2$C$\underline{H}_2$OC$_6$H$_3$), 3.915 (s, 3H, 2"-OCH$_3$), 2.14 (m, 4H, 5-OCH$_2$C$\underline{H}_2$C$\underline{H}_2$CH$_2$OC$_6$H$_3$); MS (70 eV) m/z: 425 (24%, M$^+$), 395 (11%, [C$_{22}$H$_{19}$O$_7$]$^+$), 257 (12%), 224 (100%), 202 (44%, [C$_{11}$H$_6$O$_4$]$^+$), 182 (68%,), 174, (26% [202-CO]$^+$), 145 (18%,

[174-CO]$^+$); Molecular weight calculated for $C_{22}H_{19}NO_8$: 425.1110; Found by high resolution

mass spectrometry: 425.1112

5-(4-[4-Methyl-2-nitrophenoxy]butoxy)psoralen (PAP-11). 5-(4-Chlorobutoxy)psoralen (500

mg, 1.7 mmol) and sodium iodide (741 mg, 4.9 mmol) were refluxed in 15 ml of acetonitrile for

60 min to obtain the iodo derivative. To this solution were added 2-nitro-p-cresol (523 mg, 3.4

mmol), potassium carbonate (4.0 g) and 10 ml of acetonitrile. The mixture was refluxed for 69 h.

The solid residue was re-crystallized from a methanol/acetone (80:20) mixture (447 mg, 64.0%):

m.p. = 124.5^{o}C; ^{1}H-NMR (500 MHz, CDCl$_3$): δ [ppm] = 8.14 (d, 1H, ^3J = 9.7 Hz, 3-H), 7.63 (d,

1H, ^4J = 1.8 Hz, 3"-H), 7.59 (d, 1H, ^3J = 2.4 Hz, 5'-H), 7.31 (d, 1H, ^3J = 8.2 Hz, 5"-H), 7.14 (s,

1H, 8-H), 6.98 (d, 1H, ^3J = 2.5 Hz, 4'-H), 6.96 (d, 1H, ^3J = 8.76 Hz, 6"-H), 6.26 (d, 1H, ^3J = 9.8

Hz, 4-H), 4.56 (t, 2H, ^3J = 5.7 Hz, 5-OC$\underline{H}_2$CH$_2$CH$_2$CH$_2$OC$_6$H$_3$), 4.17 (t, 2H, ^3J = 6.0 Hz, 5-

OCH$_2$CH$_2$CH$_2$C$\underline{H}_2$OC$_6$H$_3$), 2.34 (s, 3H, 4"-CH$_3$), 2.05 (m, 4H, ^3J = 4.216 Hz, 5-

OCH$_2$C$\underline{H}_2$C$\underline{H}_2$CH$_2$OC$_6$H$_3$); MS (70 eV) m/z: 409 (22%, M$^+$), 379 (20%, [C$_{22}$H$_{19}$O$_6$]$^+$), 257

(90%), 224 (100%), 202 (86%, [C$_{11}$H$_6$O$_4$]$^+$), 174, (52%, [202-CO]$^+$), 145 (30%, [174-CO]$^+$);

Molecular weight calculated for $C_{22}H_{19}NO_7$: 409.1161; Found by high resolution mass

spectrometry: 409.1170

5-(4-[2-Nitrophenoxy]butoxy)psoralen (PAP-12). 5-(4-Chlorobutoxy)psoralen (500 mg, 1.7

mmol) and sodium iodide (512 mg, 3.4 mmol) were refluxed in 15 ml of acetonitrile for 1 h to

obtain the iodo derivative. To this solution were added 2-nitrophenol (475 mg, 3.4 mmol),

potassium carbonate (4.0 g) and 15 ml of acetonitrile. The mixture was refluxed for 29 h. The

solid residue was re-crystallized from a methanol/acetone (80:20) mixture (380 mg, 56.3%): m.p.

= 121.8^{o}C; ^{1}H-NMR (500 MHz, CDCl$_3$): δ [ppm] = 8.14 (d, 1H, ^3J = 9.7 Hz, 3-H), 7.82-7.86

(overlapping dd, 2H, ^4J = 1.6 Hz, ^3J = 8.3 Hz, ^3J = 7.9 Hz, 3"-H, 6"-H), 7.60 (d, 1H, ^3J = 2.5 Hz,

5'-H), 7.52-7.55 (t, 2H, ^3J = 7.6 Hz, ^4J = 1.0 Hz, 3"-H, 4"-H), 7.15 (s, 1H, 8-H), 6.99 (d, 1H, ^3J =

2.4 Hz, 4'-H), 6.26 (d, 1H, ^3J = 9.7 Hz, 4-H), 4.57 (t, 2H, ^3J = 5.8 Hz, 5-

OC$\underline{H}_2$CH$_2$CH$_2$CH$_2$OC$_6$H$_4$), 4.23 (t, 2H, ^3J = 2.8 Hz, 5-OCH$_2$CH$_2$CH$_2$C$\underline{H}_2$OC$_6$H$_4$), 2.09-2.16 (m,

4H, 5-OCH$_2$C$\underline{H}_2$C$\underline{H}_2$CH$_2$OC$_6$H$_4$); MS (70 eV) m/z: 395 (36%, M$^+$), 365 (14%, [M-30]$^+$), 332

(78%), 283 (8%), 202 (9%, [C$_{11}$H$_6$O$_4$]$^+$), 194 (60%, [C$_{10}$H$_{12}$NO$_3$]$^+$), 122 (48%), 109 (8%), 92

(10%); Molecular weight calculated for C$_{21}$H$_{20}$O$_5$: 395.10050; Found by high resolution mass

spectrometry: 395.10053.

5-(4-[3-Nitrophenoxy]butoxy)psoralen (PAP-13). 5-(4-Chlorobutoxy)psoralen (500 mg, 1.7

mmol) and sodium iodide (512 mg, 3.4 mmol) were refluxed in 15 ml of acetonitrile for 1 h to

obtain the iodo derivative. To this solution were added 3-nitrophenol (475 mg, 3.4 mmol),

potassium carbonate (4.0 g) and 15 ml of acetonitrile and the mixture refluxed for 29 h. The solid

residue was re-crystallized from a methanol/acetone (80:20) mixture (286 mg, 42.4%): m.p. =

140.3^{o}C; ^{1}H-NMR (500 MHz, CDCl$_3$): δ [ppm] = 8.15 (d, 1H, ^3J = 9.7 Hz, 3-H), 7.84 (dd, 1H, ^3J

= 8.1 Hz, ^4J = 1.6 Hz, 4"-H), 7.61 (d, 1H, ^3J = 2.3 Hz, 5'-H), 7.42 (t, 1H, ^3J = 8.3 Hz, 5"-H), 7.41

(t, 1H, ^4J = 2.2 Hz, 2"-H), 7.22 (dd, 1H, ^3J = 8.1 Hz, ^4J = 2.3 Hz, 6"-H) 7.16 (s, 1H, 8-H), 6.97

(d, 1H, ^3J = 2.2 Hz, 4'-H), 6.27 (d, 1H, ^3J = 9.8 Hz, 4-H), 4.56 (t, 2H, ^3J = 5.8 Hz, 5-

OC$\underline{H}_2$CH$_2$CH$_2$CH$_2$OC$_6$H$_4$), 4.16 (t, 2H, ^3J = 5.6 Hz, 5-OCH$_2$CH$_2$CH$_2$C$\underline{H}_2$OC$_6$H$_4$), 2.12 (m, 4H,

5-OCH$_2$C$\underline{H}_2$C$\underline{H}_2$CH$_2$OC$_6$H$_4$); MS (70 eV) m/z: 395 (32%, M$^+$), 365 (14%, [M-30]$^+$), 292 (56%),

202 (100%, [C$_{11}$H$_6$O$_4$]$^+$), 194 (28%, [C$_{10}$H$_{12}$NO$_3$]$^+$), 174 (48%, [202-CO]$^+$), 145 (16%, [174-

CO]$^+$), 109 (8%, [C$_6$H$_5$O$_2$]$^+$), 93 (14%, C$_6$H$_5$O); Molecular weight calculated for C$_{21}$H$_{17}$NO$_7$:

395.10050; Found by high resolution mass spectrometry: 395.10103.

5-(4-[2,4-Dinitrophenoxy]butoxy)psoralen (PAP-14). 5-(4-Chlorobutoxy)psoralen (500 mg,

1.7 mmol), sodium iodide (512 mg, 3.4 mmol), 2,4-dinitrophenol (629 mg, 3.4 mmol) and

potassium carbonate (3.0 g) were refluxed in 30 ml of acetonitrile for 50 h. The solid residue was recrystallized from a methanol/acetone (80:20) mixture (82 mg, 11.0%): m.p. = 134.2°C; ^{1}H-NMR (500 MHz, CDCl$_3$): δ [ppm] = 8.78 (d, 1H, ^4J = 2.8 Hz, 3″-H), 8.45 (dd, 1H, ^3J = 9.0 Hz, ^4J = 2.8 Hz, 5″-H), 8.15 (d, 1H, ^3J = 9.7 Hz, 3-H), 7.61 (d, 1H, ^3J = 2.0 Hz, 5′-H), 7.22 (d, 1H, ^3J = 9.5 Hz, 6″-H), 7.17 (s, 1H, 8-H), 6.98 (d, 1H, ^3J = 2.1 Hz, 4′-H), 6.29 (d, 1H, ^3J = 9.8 Hz, 4-H), 4.57 (t, 2H, ^3J = 5.3 Hz, 5-OC$\underline{H}_2$CH$_2$CH$_2$CH$_2$OC$_6$H$_3$), 4.36 (t, 2H, ^3J = 5.1 Hz, 5-OCH$_2$CH$_2$CH$_2$C$\underline{H}_2$OC$_6$H$_3$), 2.2 (m, 4H, 5-OCH$_2$C$\underline{H}_2$C$\underline{H}_2$CH$_2$OC$_6$H$_3$); MS (70 eV) m/z: 440 (44%, M$^+$), 384 (18%, M$^+$-[C$_2$H$_2^+$NO]), 283 (16%), 202 (100%, [C$_{11}$H$_6$O$_4$]$^+$), 174 (34%, [202-CO]$^+$), 145 (12%, [174-CO]$^+$); Molecular weight calculated for C$_{21}$H$_{16}$N$_2$O$_9$: 440.08558; Found by high resolution mass spectrometry: 440.08598.

5-(4-Phenoxybutoxy)-4′,5′-dihydropsoralen (AS-77). PAP-1 (175 mg, 0.5 mmol) was dissolved in 40 ml of ethanol and after addition of 80 mg of 10% palladium on carbon agitated in a hydration bomb for 5 h under 2.1 bar of pressure. The Pd/C was then filtered off, the solution evaporated and the remaining residue purified by medium pressure lipid chromatography with cyclohexane/ethylacetate (80:20). Yield: (110 mg, 62.9%); m.p. = 93°C; ^{1}H-NMR (300 MHz, DMSO-d_6): δ [ppm] = 7.99 (d, 1H, ^3J = 9.7 Hz, H-4), 7.25-7.30 (m, 2H, 5-OCH$_2$(CH$_2$)$_2$CH$_2$OC$_6$$\underline{H}_5$), 6.90-6.94 (m, 3H, 5-O-CH$_2$(CH$_2$)$_2$CH$_2$-O-C$_6$$\underline{H}_5$), 6.13 (d, 1H, ^3J = 9.7 Hz, H-3), 6.53 (s, 1H, H-8), 4.63 (t, 2H, ^3J = 8.5 Hz, H-5′), 4.31 (s, 2H, 5-OC$\underline{H}_2$(CH$_2$)$_2$CH$_2$OC$_6$H$_5$), 4.05 (s, 2H, 5-OCH$_2$(CH$_2$)$_2$C$\underline{H}_2$OC$_6$H$_5$), 3.42 (t, 2H, ^3J = 8.5 Hz, H-4′), 1.91 (s, 4H, 5-OCH$_2$(C$\underline{H}_2$)$_2$CH$_2$OC$_6$H$_5$); MS (70 eV) m/z: 352 (18%, M$^+$), 204 (4%, [C$_{11}$H$_8$O$_4$]$^+$), 176 (6%, [204-CO]$^+$), 149 (65%, [C$_{10}$H$_{13}$O]$^+$), 107 (100%, [C$_6$H$_5$OCH$_2$]$^+$), 95 (5%), 77 (28%, [C$_6$H$_5$]$^+$), 55 (25%, [C$_4$H$_7$]$^+$); Molecular weight calculated for C$_{21}$H$_{20}$O$_5$: 352.13107; Found by high resolution mass spectrometry: 352.13091.

MOLPHARM/2005/15669

Log P Values. LogP (log of octanol-water partition coefficient, a measure of the hydrophobicity) values of compounds were determined by HPLC with a Waters 1525 binary HPLC pump (Milford, MA), a Kromasil 100 C18 column (5 μM, 60 x 4.6 mm; EKA Chemical Separation Products, Bohus, Sweden), and a Waters 2475 multi-wavelength fluorescence detector. Compounds were eluted with a gradient changing from 30% acetonitrile and 70% Soerensen's phosphate buffer, 11 mM, pH 7.4 to 78% acetonitrile and 22% buffer over 70 min. 4-Methylbenzaldehyde, toluene, ethyl-, n-propyl-, n-butyl-, n-pentyl-, n-hexyl-, n-heptyl and n-octylbenzene were used as standards.

Cells, cell lines and clones. Throughout the paper we are using the new IUPHAR nomenclature for ion channels (Gutman et al., 2003). Cells stably expressing *mKv1.1*, *rKv1.2*, *mKv1.3*, *hKv1.5* and *mKv3.1* have been previously described (Grissmer et al., 1994). Cell lines stably expressing other mammalian ion channels were gifts from several sources: *mKv1.7* in CHL cells and *hKCa2.3* in COS-7 cells (Aurora Biosciences Corp., San Diego, CA); *hKv1.4* and *rKv4.2* in LTK cells (Michael Tamkun, Univ. Colorado, Boulder); *hKv2.1* in HEK293 cells (James Trimmer, UC Davis); *Kv11.1* (HERG) in HEK293 cells (Craig January, Univ. Wisconsin, Madison); *hKCa1.1, rKCa2.1* and *hKCa3.1* in HEK293 cells (Khaled Houamed, Univ. Chicago, IL); *hNav1.4* in HEK-293 cells (Frank Lehmann-Horn, Univ. Ulm, Germany) and *Cav1.2* in HEK-293 cells (Franz Hofmann, Munich, Germany). RBL-2H3 (expressing *Kir2.1*) and N1E-115 neuroblastoma cells (expressing *Nav1.2*) were obtained from ATCC. *hKv1.6* and *rKv3.2* (both in pcDNA3) were obtained from Protinac GmbH (Hamburg, Germany) and transiently-transfected into COS-7 cells with Fugene-6 (Roche) according to the manufacturer's protocol. The *hKv1.3*-H399T and A413C mutants were a generous gift from Tobias Dreker and Stephan Grissmer

27

(Univ. Ulm, Germany), while the H399Y and A413V (Panyi et al., 1995) mutants were kindly

supplied by Carol Deutsch (Univ. Pennsylvania, PA).

Electrophysiology. All compounds used for electrophysiological testing were >98% pure as

determined by combustion analysis. All experiments were conducted in the whole-cell

configuration of the patch-clamp technique with a holding potential of -80 mV unless otherwise

stated. Pipette resistances averaged 2.0 MΩ, and series resistance compensation of 80% was

employed when currents exceeded 2 nA. Kv1.3 currents were elicited by repeated 200-ms or 2-

sec pulses from -80 mV to 40 mV, applied at intervals of 30 or 60 s. Kv1.3 currents were

recorded in normal Ringer solution with a Ca^{2+}-free pipette solution containing (in mM): 145

KF, 10 HEPES, 10 EGTA, 2 $MgCl_2$, pH 7.2, 300 mOsm. EC_{50}-values and Hill coefficient were

determined by fitting the Hill equation to the reduction of area under the current curve measured

at 40 mV. Kv1.1, Kv1.5, Kv1.4, Kv1.6, Kv1.7, Kv2.1, Kv3.1, Kv3.2 and Kv4.2 currents were

recorded with 200-ms depolarizing pulses to 40 mV applied every 10 sec (Bardien-Kruger et al.,

2002; Grissmer et al., 1994; Wulff et al., 2000). For Kv1.2 we applied 200-ms pulses to 40 mV

every 5 sec to allow for the channel's use-dependent activation (Grissmer et al., 1994). HERG

(*Kv11.1*) currents were recorded with a 2-step pulse from -80 mV first to 20 mV for 2 sec and

then to -50 mV for 2 sec (Zhou et al., 1998) and the reduction of both peak and tail current by

the drug was determined.

The inward rectifier (*rKir2.1*) in RBL cells was studied with ramp pulses from -150 to 0

mV applied every 10 sec and a Na^+ aspartate Ringer external and a K^+ aspartate-based pipette

solution containing 50 nM free Ca^{2+}. For measurements of IK_{Ca} (*KCa3.1*) SK_{Ca} (*KCa2.3*) and

BK_{Ca} (*KCa1.1*) currents we used an internal pipette solution containing (in mM): 145 K^+

aspartate, 2 $MgCl_2$, 10 HEPES, 10 K_2EGTA and 8.5 $CaCl_2$ (1 μM free Ca^{2+}), pH 7.2, 290-310 mOsm, and an external solution containing (in mM): 160 Na^+ aspartate, 4.5 KCl, 2 $CaCl_2$, 1 $MgCl_2$, 5 HEPES, pH 7.4, 290-310 mOsm. BK_{Ca} currents were elicited by 200-ms voltage ramps from −80 to 80 mV applied every 10 sec, and channel block measured as reduction of slope conductance at 35 mV. IK_{Ca} and SK_{Ca} currents were elicited by 200-ms voltage ramps from −120 mV to 40 mV applied every 10 sec and the reduction of slope conductance at −80 mV by drug taken as a measure of channel block (Wulff et al., 2000). Nav1.2 currents from N1E-115 cells and Nav1.4 currents from stably transfected HEK cells were recorded with 100 ms pulses from −80 mV to 0 mV every 10 sec with a KCl-based pipette solution and normal Ringer as an external. Cav1.2 currents were elicited by 600-ms depolarizing pulses from −80 to 20 mV every 10 sec with a CsCl based pipette solution and an external solution containing 30 mM $BaCl_2$ (Kolski-Andreaco et al., 2004). Blockade of both Na^+ and Ca^{2+} currents was determined as reduction of the current minimum. Swelling-activated chloride currents were elicited from activated human T cells with a hyperosmolar Cs glutamate based pipette solution (420 mOsm) and ramp pulses from −120 to 60 mV every 10 sec (Ross et al., 1994).

Cytotoxicity assays. Jurkat E61 and MEL cells were seeded at 5×10^5 cells/ml in twelve-well plates. Compounds were added at concentrations of 10 nM, 100 nM and 10 μM in a final DMSO concentration of 0.1%, which was found not to affect cell viability. After 48 h the cells in each well were well mixed and resuspended and the number of trypan blue positive cells in 3 aliquots from each well determined under a light microscope. The test was repeated twice.

Ames test. The mutagenic activity of PAP-1 was determined on the *Salmonella typhimurium* tester strains TA97A, TA98, TA100, TA102 and TA1535 by Nelson Laboratories (Salt Lake City, UT).

Receptor Screening: PAP-1 was screened at 1 µM for potential affinity to a panel of 56 receptors by displacement of standard radioligands at MDS Pharma (http://www.mdsps.com). The following receptors were included: adenosine (A_1, A_{2A}, A_3), adrenergic (α_{1A}, α_{1B}, α_{1D}, α_{2A}, β_1, β_2), bradykinin (B_1, B_2), dopamine (D_1, D_{25}, D_3, $D_{4.2}$), endothelin (ET_A, ET_B), epidermal growth factor, estrogen (ERα), GABA$_A$ (agonist site), GABA$_B$ (benzodiazepine and non-selective), glucorticoid, glutamate (kainate, NMDA agonism, NMDA glycine, NMDA phencyclidine), histamine (H_1, H_2, H_3), imidazoline (I_2), interleukin-1, leukotriene (CysLT1), muscarinic (M_1, M_2, M_3), neuropeptide Y (Y_1, Y_2), nicotinic acetylcholine, opiate (δ, κ, μ), phorbol ester, platelet activating factor, purinergic (P_{2X}, P_{2Y}), serotonin (5-HT$_{1A}$, 5-HT$_3$), sigma (σ_1, σ_2), tachykinin (NK$_1$), testosterone, transporters (dopamine, GABA, norepinephrine, serotonin). Since significant activity was only witnessed on the dopamine transporter PAP-1 was retested at 0.01, 0.1, 0.25 and 1 µM in order to determine an IC$_{50}$ and a Hill coefficient. All assays were performed in duplicate.

Inhibition of cytochrome P450 dependent enzymes. Inhibition of the catalytic activity of purified recombinant human cytochrome P450 2A6 and 3A4 in microsomes (BD Gentest Products and Services, Woburn, MA) was assayed on the turnover of coumarin (CYP2A6) or 7-benzyloxy-4-trifluoromethyl-coumarin (CYP3A4) by the detection of their fluorescent metabolites (Henderson et al., 1999) and IC$_{50}$ values determined by testing multiple compound

30

concentrations ranging from 10 nM to 200 µM. All experiments were conducted in duplicate and results are reported as percent inhibition. Tranylcypramine (CYP2A6) and ketoconazole (CYP3A4) were run as positive controls on the same plates and rendered IC$_{50}$ values of 170 nM and 37 nM, respectively.

DNA-crosslinking. The DNA-crosslinking potency of selected compounds was determined by measuring melting profiles of poly(dA-dT)-poly(dA-dT) DNA in the presence and absence of compound with and without UVA irradiation according to Dall`Acqua *et al.* (Dall' Acqua et al., 1971). Incubation mixtures containing 10 µM of the compound, 0.1 units of poly(dA-dT)-poly(dA-dT) (Sigma-Aldrich, Deisenhofen, Germany) and 1% DMSO and MOPS (3-morpholinopropanesulfonic acid) buffer (0.1 M; pH 7.2) were prepared in 2 ml quartz cuvettes. Samples were irradiated with a Heraeus Fluotest lamp for 30 min at a distance of 20 cm with an intensity of 3.5 mW/cm^2 or stored in the dark for 30 min. Afterwards samples were placed into HP 8845A Dioden-Array spectrophotometer fitted with a Julabo F20-C heating controller. The temperature was directly measured in the cuvettes with a digital thermometer. Heating was applied at a rate of 1 °C min^{-1}, with absorbance (260 nm) and temperature data sampling at 1-min intervals until the temperature reached 80 °C.

Photoproduction of singlet oxygen. The production of singlet oxygen (^{1}O$_2$) by selected psoralen compounds was determined according to Kraljic and El Moshni (Kraljic and El Moshnie, 1978). 10 µM of compound were mixed with 4 µM *N,N*-dimethyl-4-nitrosoaniline, 10 mM histidine and 1% methanol in oxygen-saturated phosphate buffer (0.01 M; pH 7.0) and irradiated with a Heraeus Fluotest lamp for 5 h at a distance of 20 cm with an intensity of 3.5

mW/cm^2. Singlet oxygen mediated photobleaching of the yellow *N,N*-dimethyl-4-nitrosoaniline was followed by photometric measurements (440 nm) every 30 min. Results are given as % reduction of initial absorption at 440 nM before irradiation and are corrected for "self bleaching" in the absence of compounds (11.4% ± 0.3 %, n = 9).

Proliferation assays. Untouched CD3$^+$ T cells were isolated from peripheral blood of healthy volunteers with RosetteSep (StemCell Technologies, Vancouver) and then incubated with a biotinylated anti-CCR7 Ab (BD Pharmigen, Clone 3D12). After two washes with PBS the labeled cells were first incubated with an anti-biotin tetramer complex (StemCell Technologies, Vancouver) and then with magnetic micro-beads. The cells were placed onto a negative selection column in a magnet (all StemCell Technologies) and pure CCR7$^-$ cells were eluted (97% CCR7$^-$ as determined by flow cytometry). CCR7$^-$ T cells were then seeded at 5x10^4 per well together with 5x10^4 autologous irradiated PBMCs (2500 rad) in RPMI culture medium into round bottom 96-well plates. PAP-1 was added at different concentrations and the cells were stimulated with 25 ng/ml soluble anti-CD3 Ab (Biomeda) 30 min later. To determine the effect of PAP-1 on naïve and central memory T cells, human PBMCs were seeded at 2x10^5 cells per well in flat-bottom 96-well plates, pre-incubated with increasing concentrations of PAP-1 for 30 min and then stimulated with 25 ng/ml anti-CD3 mAb (Biomeda). [^{3}H]-TdR (1 µCi per well) was added for the last 12 h of the 60-h assay. Cells were harvested onto glass fiber filters and radioactivity measured in a β–scintillation counter.

DTH. Nine to eleven week old female Lewis rats were purchased from Charles River (Wilmington, MA) and housed in microisolator cages with irradiated rodent chow and autoclaved water *ad libitum*. All experiments were in accordance with NIH guidelines and

approved by the University of California, Davis, Institutional Animal Care and Use Committee.

Rats were immunized at the base of the tail with 200 µl of an emulsion of egg albumin grade II

(Sigma) in complete Freund's adjuvant (Difco, Detroit, MI). The emulsion was prepared with 50

% CFA and 50% saline containing a final concentration of 1 mg/ml albumin. Seven days later,

the thickness of both ears was measured using a spring-loaded micrometer (Mitutoyo, Spokane,

WA). The rats were then challenged by an injection of 10 µl of albumin (2 mg/ml) dissolved in

saline in the pinna of one ear and saline in the other ear. In two experiments rats received i.p.

injections of 0.3, 1.0 or 3.0 mg/kg of PAP-1 or of vehicle (saline with 25% Cremophor EL

(Sigma)) 3x daily for 48 hours starting 24 hours before the challenge. In another experiment rats

were gavaged 3x daily with peanut oil or 5, 20 or 80 mg/kg PAP-1 dissolved in peanut oil

(volume 0.5 ml). Ear swelling was measured 24 hours later. Values are given as differences in

the thickness (µm) of the albumin injected ear measured before the challenge and 24 h later. The

other ear was used as a control for the injection and the rats were discarded from the experiment

if the thickness of the saline injected ear increased more than 10%.

Results

Probing of the Alkoxypsoralen Pharmacophore to Increase Selectivity for Kv1.3 over Kv1.5. Using 5-MOP as a template we previously developed a series of 5-phenylalkoxypsoralens (= Psora series) that inhibited Kv1.3 with low nM affinity (Vennekamp et al., 2004) and found that the essential pharmacophore of this class of Kv1.3 blockers consisted of a psoralen moiety that is attached through a ~7Å long alkyl chain linker in the 5-position to a phenyl ring. We further postulated that the Psora compounds bind to the Kv1.3 channel protein via two π-π electron interactions, one involving the psoralen core and the second involving the side chain phenyl ring. Psora-4, the most potent compound of this series, blocked Kv1.3 with an EC_{50} of 3 nM and displayed good selectivity over other Kv channels with the exception of Kv1.5 (EC_{50} 7.7 nM) (Vennekamp et al., 2004). Since Kv1.5 encodes the ultra-rapid delayed rectifier current (I_{Kur}) in the human heart (Fedida et al., 1993) we were concerned about potential cardiac side-effects when using Psora-4 as an immunosuppressant and decided to start a new medicinal chemistry effort centered around Psora-4 in order to improve the selectivity for Kv1.3 over Kv1.5. Towards this aim we pursued three synthetic strategies (Figure 1B): In strategy-**a,** we replaced the side-chain phenyl ring with π-electron rich aliphatic substituents or heteroaromatic ring systems. In strategy-**b,** we introduced polar functionalities into the linker such as an ether (O) or a carbonyl (CO) moiety in order to make the linker more hydrophilic by adding an additional hydrogen acceptor. In strategy-**c,** we planned to alter the electron density in the side-chain phenyl ring by introducing electron-withdrawing or electron-donating substituents. The chemical identity and purity of all newly synthesized compounds was confirmed by ^{1}H and ^{13}C-NMR, mass spectrometry and combustion analysis before they were tested in whole-cell patch-

clamp experiments for their potency to block Kv1.3 and Kv1.5 stably expressed in L929 or MEL cells.

Strategy-a: Introduction of π-Electron Rich Aliphatic Substituents or Heteroaromatic Rings. Substitution of the phenyl ring with π-electron rich aliphatic groups such as cyano as in ACP-3 or alkyne as in AP-1 resulted in a 100-1000 fold reduction in potency on Kv1.3 and no significant improvement in selectivity over Kv1.5 (Figure 1B and 2). This result suggested that in addition to possessing π-electron density the side-chain substituent also has to have a certain minimum bulk. We therefore next tried replacing the side-chain phenyl ring with bulkier heterocyclic ring systems (Figure 1B and 2). In general this strategy rendered compounds of reduced affinity to Kv1.3 and the most obvious conclusion about the structure-activity relationship (SAR) we could draw from this set of compounds was that the introduction of polar heterocycles as in PAP-17a and PP-1 or of a basic nitrogen atom, that is charged at physiological pH as in PH-3, is extremely detrimental and reduces the affinity of the compounds to Kv1.3 into the low micromolar range. PH-3 constitutes a combination of Psora-4 and the classical K^+ channel blocker 4-aminopyridine in one molecule. Its 4'-aminogroup (Figure 1B) is a secondary amine and has a pKa value of 8.0 meaning that at a pH of 7.4 roughly 20% of the molecule will exist as the free base and 80% will be protonated. The free base molecules can easily cross the plasma membranes in whole-cell patch-clamp experiments and are likely to be reprotonated at the intracellular pH of 7.2 resulting in only 14% free base and 86% charged molecules in the cytoplasm. Based on this we postulate that PH-3 is such a weak Kv1.3 blocker because the protonated molecules are not able to bind to the lipophilic alkoxypsoralen binding site, which is very probably located on the intracellular side of the Kv1.3 protein (Vennekamp et al., 2004;

Wulff et al., 1998). This hypothesis is supported by the fact that the two pyrimidines PH-9 and PAP-17 (Figure 1B and Figure 2 top), which are very similar in size and π-electron density to PH-3 but which contain no basic nitrogen atom, are much more potent Kv1.3 blockers with EC_{50} values of 50 and 125 nM, respectively. However, the selectivity of all pyridine or pyrimidine substituted compounds over Kv1.5 was extremely poor (0-3 fold).

In contrast, when we replaced the phenyl ring with a 5-membered pyrazole (PH-1, EC_{50} 450 nM) or thiadiazole ring (PH-4, EC_{50} 175 nM), or a larger, oxygen-rich coumarin ring (PH-5, EC_{50} 125 nM) the compounds exhibited 10-40 fold selectivity for Kv1.3 over Kv1.5 (Figure 2 top) despite their ~100-fold loss in activity in comparison to Psora-4. However, in PH-4 and PH-5 we had also simultaneously introduced an oxygen or a sulfur atom into the side-chain right next to the heterocycle and it was therefore not clear whether the heterocycle or this additional heteroatom in the linker, which constitutes an additional hydrogen bond acceptor, was responsible for the gain in selectivity for Kv1.3 over Kv1.5. In order to dissect this question we next synthesized a series of compounds where we introduced an oxygen atom into the linker but kept Psora-4's side-chain phenyl ring intact (see Strategy-**b** in Figure 1B).

Strategy-b: Introduction of Polar Functionalities into the Linker. The first observation we made when following this strategy was that the compounds were much more potent Kv1.3 blockers (EC_{50}s of 2 to 50 nM) than when we introduced oxygen or sulfur atoms and simultaneously replaced the phenyl ring with heterocycles demonstrating that a phenyl ring constitutes the optimal ring system in the side-chain. While replacing one of the methylene groups in the linker with a ketone moiety as in KP-1 (Figure 2 middle) did not improve selectivity over Kv1.5, introduction of an ether oxygen adjacent to the phenyl ring as in PAP-1

(Figure 2 middle) increased both the potency for Kv1.3 (EC$_{50}$ 2 nM) and the selectivity over

Kv1.5 (EC$_{50}$ 45 nM). Since PAP-1 was 23-fold selective over Kv1.5 we subsequently

synthesized a series of phenoxyalkoxypsoralens (PAPs) where we varied the length of the linker

or changed the exact position of the ether oxygen atom (Figure 2 middle). Similar to our

previously described Psora series (Vennekamp et al., 2004) the potency of the PAP compounds

depended on the length of the linker but the optimal length proved to be ~8 Å like in PAP-1

instead of ~7 Å like in Psora-4. Shorter and longer linkers like in PAP-3 (EC$_{50}$ 15 nM) and AS-

121 (EC$_{50}$ 15 nM) decreased both potency and selectivity compared to PAP-1 (Figure 3).

Moving the oxygen from position-4 of the linker in PAP-1 to position-3 in PAP-5, PAP-6 and

PAP-7 also reduced both potency and selectivity for Kv1.3 (Figure 2). We therefore concluded

that an 8 Å long aliphatic linker with an ether oxygen atom adjacent to the phenyl ring

constituted an optimum in terms of both potency and selectivity.

Strategy b + c: Introduction of Substituents into the Side-chain Phenyl Ring of PAP-1.

Since PAP-1 exhibited a much higher selectivity for Kv1.3 (EC$_{50}$ 2 nM) over Kv1.5 (EC$_{50}$ 45

nM) than Psora-4, we changed our synthetic strategy and altered the π-electron density in the

side-chain phenyl ring of PAP-1 instead of Psora-4 as originally planned and thus combined

strategies **b** and **c** (Figure 1B and 2). Electron donating groups (-OCH$_3$, -CH$_3$, -CF$_3$) in general

slightly decreased the potency of the compounds on Kv1.3 (EC$_{50}$s 7-65 nM) but "destroyed" the

selectivity over Kv1.5 (see AS-67, AS-68, AS-96, AS-118 in Figure 2). The effects of electron

withdrawing groups (-NO$_2$, -Cl) on potency and selectivity were more complicated and depended

on the chemical nature of the groups and on the exact position in which they were introduced.

The halogen atoms fluorine (AS-111) and chlorine (AS-84) had very little effect on the potency

for Kv1.3 with EC_{50} values of 12 and 5 nM, respectively, but drastically reduced the selectivity over Kv1.5 (Figure 2). Introduction of the strongly electron-withdrawing nitro group in the 4-position as in AS-78 resulted in 15-fold selectivity for Kv1.3 (EC_{50} 5 nM) over Kv1.5 (EC_{50} 105 nM) (Figure 2). However, shifting the nitro group to the 2-position as in PAP-12 (EC_{50} 61 nM) or to the 3-position as in PAP-13 (EC_{50} 81 nM) reduced both potency and selectivity significantly (Figure 3). The introduction of two nitro groups in the 2- and the 4-position as in PAP-14 also did not prove beneficial and further lowered the EC_{50} for Kv1.3 to 140 nM (Figure 2).

The simultaneous introduction of both an electron withdrawing nitro group and an electron donating methoxy (PAP-10) or methyl group (PAP-11) dramatically reduced the potency of the compounds but interestingly reversed the selectivity. While PAP-10 showed only a marginal preference for Kv1.5, PAP-11 blocked Kv1.5 (EC_{50} 248 nM) three times more potently than Kv1.3 (EC_{50} 700 nM). If selective Kv1.5 blockers can be developed out of PAP-11 will be the focus of future experiments and double substitutions were not pursued further in this SAR study.

Introduction of a bulky phenoxy group in position-4 of the side chain phenyl ring as in AS-85 (Figure 2) decreased the EC_{50} for Kv1.3 8-fold to 16 nM but increased the selectivity over Kv1.5 to 45-fold (EC_{50} Kv1.5 750 nM). The fact that both the bulky AS-85 (volume 1367 Å^3) and the coumarin ring substituted PH-5 (Figure 1B) displayed such good selectivity suggests that the alkoxypsoralen binding site is wider in Kv1.3 than in Kv1.5. With the synthesis of AS-77 we lastly tested which effect hydration of the furan ring in the psoralen system of PAP-1 has and found that it reduced both the potency (EC_{50} 22 nM) and the selectivity (Figure 2).

MOLPHARM/2005/15669

PAP-1 and AS-85 Constitute Promising New Kv1.3 Blockers: Of the newly synthesized compounds in this study PAP-1 constitutes the most promising compound. It inhibits Kv1.3 with an EC_{50} of 2 nM (Figure 3), exhibits 23-fold selectivity over Kv1.5 and has a logP value of 4.03, and thus the right physicochemical properties in order to be potentially orally available. Despite its higher selectivity over Kv1.5 (45-fold) the phenoxy-substituted AS-85 is not a good drug candidate because its high lipophilicity (logP 5.03) violates the Lipinski "rule of five", which states that a potential small molecule drug should have a molecular weight below 500, a log P value below 5, less than 5 hydrogen bond donors and less than 10 hydrogen bond acceptors in order to be orally available (Lipinski et al., 1997). However, its high logP value could make AS-85 an interesting compound for topical application in the treatment of psoriasis and other autoimmune diseases of the skin.

Selectivity of PAP-1 over Other Ion Channels. PAP-1, the most potent of our new compounds, blocked both cloned (EC_{50} 2.0 ± 0.2 nM) and native Kv1.3 channels in human T cells (EC_{50} 2.1 ± 0.2 nM) with a Hill coefficient of 2 (Figure 3B), indicating that two PAP-1 molecules interact with one channel molecule. In contrast to its parent compound Psora-4 (Vennekamp et al., 2004), PAP-1 displayed 23-fold selectivity over the cardiac potassium channel Kv1.5 suggesting that it could be used as an immunosuppressant without causing cardiac side effects. In order to test that we did not pick up affinity to any other ion channels while optimizing for selectivity over Kv1.5, we further screened PAP-1 on a panel of 22 K^+, Na^+, Ca^{2+} and Cl^- channels (Figure 3C). PAP-1 was found to be 33-fold selective over Kv1.1, 125-fold selective over Kv1.2, 37-fold selective over Kv1.4, 31-fold selective over Kv1.6 and 49-fold selective over Kv1.7. This selectivity over the closely related Kv1-family channels makes PAP-1 the most selective known small molecule

Kv1.3 blocker (Chandy et al., 2004). As expected, PAP-1 was even more selective over more distantly related channels: 490-fold over Kv3.2, 600-fold over Kv4.2 and more than 1000-fold over Kv2.1, Kv3.1, Kv11.1 (HERG), the inward-rectifier Kir2.1, the calcium-activated K^+ channels KCa1.1 (BK), KCa3.1 (IKCa1), $K_{Ca}2.1$-2.3 (SKCa1-3), the neuronal and the skeletal muscle Na^+ channels Nav1.2 and Nav1.4, the voltage-activated Ca^{2+} channel Cav1.2 (L-type) and the swelling activated chloride channel in human T cells (Figure 3C).

PAP-1 Binds to the C-type Inactivated State of Kv1.3. For our template Psora-4 we had previously found that it blocks Kv1.3 by binding to the C-type inactivated state of the channel (Vennekamp et al., 2004) and therefore suspected that PAP-1 would do the same. In order to test whether PAP-1 blocks the closed Kv1.3 channel or a post-activation state we first applied a 200-ms depolarizing pulse to elicit a control Kv1.3 current and then perfused 10 nM of PAP-1 into the bath while the channel was closed (Figure 4A). After a five-min interval to allow ample time for the lipophilic PAP-1 to diffuse into the cell and reach its binding site, we applied a second depolarizing pulse, which elicited a current of equivalent amplitude to the control current, confirming our hypothesis that PAP-1 does not bind to the closed channel. With subsequent depolarizing pulses blockade slowly developed (Figure 4A) demonstrating that multiple openings of the channel are required to reach steady-state block. This result suggested that PAP-1 blocks either the open and/or C-type inactivated state of Kv1.3. In order to distinguish between these two possibilities we performed four types of experiments (Figure 4B-F). We first varied the pulse length and found that the time to reach steady-state block depended on the duration of the depolarizing pulse. When depolarizing pulses of 200 ms to 40 mV were applied every 60 sec from a holding potential of -80 mV, 900 sec (15 pulses) was required to reach steady-state block

(Figure 4B). Lengthening the pulse duration to 2 sec and thus causing more of the channels to undergo C-type inactivation during the pulse shortened the time to reach steady-state block to 480 sec (8 pulses). In contrast, shortening the pulse duration to 2 ms prolonged the time to reach steady state block to such an extent that 10 nM PAP-1 exhibited less than 10% blockade after ~20 min (Figure 4C) because under these conditions only a small fraction of the channel ensemble undergoes C-type inactivation. However, the fact that PAP-1 blocks the C-type inactivated state became even more readily apparent when we performed the following experiment: A Kv1.3 control current was elicited through a 200-ms depolarizing pulse from −80 to 40 mV and the channels were forced into the C-type inactivated state through 5 consecutive pulses at an interval of 1 sec (Figure 4D). The membrane was then held for 5 min at −80 mV to allow the entire channel ensemble to recover from inactivation. A second set of 5 consecutive pulses was then applied to again force the channels into the C-type inactivated state and 10 nM of PAP-1 were perfused immediately afterwards. After holding the membrane at rest for 5 min virtually no Kv1.3 channels could be opened because PAP-1 had found them in the C-type inactivated state and blocked them (Figure 4D). As a final proof that PAP-1 binds to the C-type inactivated state we studied its effect under conditions where C-type inactivation is altered reasoning that this should also change the sensitivity of Kv1.3 to PAP-1. As expected, removal of C-type inactivation by 160 mM external $[K^+]_o$ (Cahalan et al., 1985; Levy and Deutsch, 1996) decreased PAP-1's potency 10-fold compared with 4.5 mM $[K^+]_o$ (Figure 4E). A similar reduction in potency was seen if C-type inactivation was removed or slowed through mutations in the outer vestibule of Kv1.3 like H399T (Figure 4F), H399Y or A413C (data not shown). In contrast, the A413V mutation, which speeds up inactivation (Panyi et al., 1995), was as sensitive to PAP-1 as the wild-type channel but equilibrium block was reached faster (data not shown).

Taken together, these results indicate that PAP-1 preferentially binds to residues in Kv1.3 that become accessible when the channel undergoes C-type inactivation. The off-binding parameters of PAP-1 were not determined because blockade by PAP-1 was irreversible unless very large volumes of DMSO containing Ringer solution were used for washout.

Toxicity Studies. In order to determine if PAP-1 can be safely used *in vivo* we performed several general toxicity studies and put PAP-1 through an industrial type "Lead Profiling Screen" for selectivity over a panel of 56 receptors. We also more specifically tested for inhibition of P450 dependent enzymes and for photoxicity because some psoralens have been reported to exhibit these properties (Averbeck, 1989; Zhang et al., 2001).

At concentrations ranging from 10 nM to 10 μM PAP-1 did not reduce the viability of Jurkat T or MEL cells as measured by trypan blue exclusion after 48 hours. At a concentration of 1 μM, which corresponds to 500x the EC_{50} for Kv1.3 blockade, PAP-1 was negative in the Ames test on five tester strains of *Salmonella typhimurium*, demonstrating that it is not mutagenic. In a specificity screen PAP-1 was tested at 1 μM for displacement of standard radioligands on 56 receptors and transporters. No significant activity was noted on any receptor or transporter with the exception of the human dopamine transporter stably expressed in CHO cells on which PAP-1 inhibited binding of the dopamine up-take inhibitor [125I]-RTI-55 with an IC_{50} of 100 nM. PAP-1 thus exhibits 50-fold selectivity over the human dopamine transporter and more than 500-fold selectivity over all other tested receptors and transporters. We further injected rats at 60 mg/kg subcutaneously with PAP-1 and witnessed no signs of acute toxicity like distress, paralysis, ataxia, seizures or weakness. However, since PAP-1 shows a significant affinity to the human

dopamine transporter we will pay close attention to side effects that might be caused by inhibition of this transporter during future toxicity tests.

Cytochrome P450 inhibition. Since psoralens like 8-methoxypsoralen and the related 6',7'-dihyroxybergamottin, a grapefruit juice constituent, have been reported to inhibit the cytochrome P450 dependent enzymes CYP2A6 or CYP3A4 (Zhang et al., 2001), we tested PAP-1, its hydrated analog AS77, AS-78, PH-9 and 5-MOP for inhibition of these two enzymes (see Table 1 for IC_{50} values). Interestingly all compounds with an aromatic furan ring (PAP-1, AS-78, PH-9 and 5-MOP) showed a higher affinity to CYP3A4, the major xenobiotic metabolizing enzyme in human liver, while the hydrated AS-77 preferentially blocked the nicotine metabolizing enzyme CYP2A6 (Table 1). However, compared with the classical CYP3A4 blocker ketoconazole (IC_{50} 37 nM in this assay) and the CYP2A6 blocker tranylcypramine (IC_{50} 175 nM) all tested psoralens were weak P450 inhibitors. Our most potent Kv1.3 blocker PAP-1 displays more than 1000-fold selectivity for Kv1.3 over CYP3A4 (IC_{50} 2.4 μM) and CYP2A6 (IC_{50} = 45 μM) and it is therefore unlikely that PAP-1 will cause any serious drug-drug interactions *in vivo* when used in combination with drugs that are metabolized through CYP3A4 or CYP2A6.

Phototoxicity. Depending on the exact orbital configuration of their valence electrons some psoralens can undergo type-I and type-II photoreactions with macromolecules in biological systems when irradiated with UVA light (Zarebska, 1994). In type-I photoreactions (= direct reactions) psoralens form photoadducts with pyrimidine bases of DNA or unsaturated fatty acids in membranes. In type-2 photoreactions, which require the presence of oxygen, psoralen molecules transfer the energy they absorb from UVA light to oxygen and generate reactive

oxygen species like singlet oxygen ($^1O_2$) which then oxidize proteins and membrane lipids. Taken together these reactions underlie the well-known phototoxic, photomutagenic and photocarcinogenic properties of 5-MOP, 8-MOP and trioxsalen, which are clinically used for PUVA (psoralen + UVA) therapy of psoriasis (Gasparro, 2000).

DNA-crosslinking. DNA modification by 8-MOP or trioxsalen is a two step process in which the planar psoralen system first intercalates into the DNA double helix and then undergoes a photoaddition reaction with a pyrimidine base, preferably thymine, under UVA irradiation (Zarebska, 1994). Since repeated adenine-thymine-sequences are described to be "hot-spots" for psoralen cross-linking (Sage and Moustacchi, 1987), we used poly(dA-dT)-poly(dA-dT) DNA to study the photoreactivity of PAP-1. Photobinding of psoralens stabilizes the DNA helix leading to an increase in thermal helix-coil transition temperature (T_m) that corresponds to the amount of cross-linking (Vedaldi et al., 1995). While PAP-1 at 10 μM induced no change in the DNA melting curve (ΔT_m = -0.5 ± 0.3°C) under UVA irradiation, the classical intercalating psoralens 5-MOP (ΔT_m = 12°C), 8-MOP (ΔT_m = 7°C) and trioxsalen (ΔT_m > 28°C) significantly increased T_m at the same concentration. This result was partly to be expected from PAP-1's structure because psoralens with large substituents are normally too bulky to intercalate into DNA.

Photoproduction of singlet oxygen. Singlet oxygen production by psoralens is typically measured through oxidative bleaching of the yellow dye *N,N*-dimethyl-p-nitrosoanilin (Kraljic and El Moshnie, 1978). In contrast to the strong singlet oxygen producer psoralen (57.4% ± 1.7 % bleaching, n = 4), we found that PAP-1 at 10 μM was only a very weak producer of singlet oxygen (7.1% ± 0.4 % bleaching, n = 3).

So in summary, PAP-1 does not exhibit the photoreactivity of other psoralens and should be free of phototoxic and photomutagenic properties *in vivo*.

PAP-1 Preferentially Suppresses the Proliferation of T_{EM} Cells. Before embarking on *in vivo* experiments with PAP-1, we tested its effect on the proliferation of human T cells. Similar to its parent compound Psora-4 (Vennekamp et al., 2004) and the Kv1.3 blocking peptides ShK and ShK(L5) (Beeton et al., 2005; Wulff et al., 2003b) we expected that PAP-1 would inhibit the proliferation of CCR7$^-$ T_{EM} cells more potently than the proliferation of bulk peripheral blood T cells that predominantly consist of naïve and T_{CM} cells. We therefore isolated CCR7$^-$ T_{EM} cells from CD3$^+$ peripheral blood T cells of three healthy volunteers by eliminating the CCR7$^+$ cells with the help of a biotinylated anti-CCR7 antibody and magnetic beads. The untouched T_{EM} cells, which were confirmed by flow cytometry to be 97% CCR7$^-$, were then stimulated to proliferate with a mitogenic anti-CD3 antibody in the presence and absence of PAP-1. For comparison we also stimulated peripheral blood mononuclear cells (PBMCs) from the same donors (74-89% CCR7$^+$) with anti-CD3 antibody in order to elicit a proliferative response that was mainly carried by naïve and T_{CM} T cells. We could not use pure CCR7$^+$ cells for these experiments because the anti-CCR7 antibody partially activated the cells that were labeled with it. As shown in Figure 5A PAP-1 suppressed the proliferation of T_{EM} with an IC$_{50}$ of 10 nM but was much less effective on PBMCs (IC$_{50}$ ~800 nM), presumably because these cells rapidly up-regulate KCa3.1 during the activation process and thus escape inhibition by Kv1.3 blockers.

PAP-1 Prevents DTH in Lewis Rats. As a final test for whether PAP-1 could be used to target T_{EM} cells in autoimmune reactions we evaluated its effectiveness in suppressing delayed type hypersensitivity (DTH) in Lewis rats. The DTH reaction constitutes a "perfect" model for evaluating Kv1.3 blockers because it is primarily mediated by skin homing CD4$^+$ T_{EM} cells

(Soler et al., 2003). We immunized female Lewis rats with ovalbumin in complete Freund's adjuvant and challenged them seven days later by an injection of ovalbumin in saline into the pinna of the left ear. The difference in ear thickness was then determined with a micrometer 24 hours later as a measure of the immune response against the ovalbumin. PAP-1 or vehicle (saline containing 25% cremophor SL) was administered intraperitonealy three times daily for 48 hours starting from the day before the challenge. As shown in Figure 5B, PAP-1 dose-dependently suppressed the DTH reaction. At 3 mg/kg PAP-1 was as effective as the peptidic Kv1.3 blocker ShK (16 μg/kg 3x daily). PAP-1 also potently suppressed DTH when administered by gavage in peanut oil, demonstrating that it is orally available (Figure 5C). As is often the case with oral administration we needed higher doses of PAP-1 to completely suppress DTH and the variations between individual rats were larger presumably because of differences in absorption and metabolism.

Discussion

Using our previously described small molecule Kv1.3 blocker Psora-4 (Vennekamp et al., 2004) as a template, we have further explored the SAR of the phenylalkoxypsoralens and have now identified a number of new phenoxyalkoxypsoralens that potently inhibit the lymphocyte K^+ channel Kv1.3 and display 2 to 50-fold selectivity over the cardiac K^+ channel Kv1.5. Our most "drug-like" new compound, PAP-1, inhibits Kv1.3 with an EC_{50} of 2 nM and is 23-fold selective over Kv1.5. PAP-1 further displays 33 to 125-fold selectivity over all other Kv1-family channels and thus constitutes currently the most potent and selective small molecule Kv1.3 blocker. All other published small molecule Kv1.3 blockers inhibit at least one of the Kv1-channels, most commonly Kv1.4 or Kv1.5, with equal affinity as Kv1.3 (Chandy et al., 2004; Wulff et al., 2003a).

Based on the results presented here and on our previous work we propose that the essential pharmacophore of the new phenoxyalkoxypsoralen (PAP) Kv1.3 blockers consists of a planar, π-electron rich three membered ring system that is connected through a roughly 8 Å long linker containing two oxygen atoms to a preferably un-substituted phenyl ring. Similar to Psora-4, the PAPs probably bind to Kv1.3 via two π-π electron interactions, one involving the psoralen moiety and the second involving the side-chain phenyl ring. Unlike Psora-4, the PAPs contain an additional O-atom in the linker, which constitutes a potential additional hydrogen bond acceptor. However, whether or not this O-atom really forms a hydrogen bond with the Kv1.3 protein is impossible to say without knowing where precisely the binding site of the PAPs is. A very interesting phenomenon with the PAPs is that the selectivity over Kv1.3 changes from no selectivity to 43-fold selectivity depending on the chemical nature, the size and the exact position of additional substituents on the side-chain phenyl ring. While the unsubstituted PAP-1 is 23-fold

selective over Kv1.5, most substituents with the exception of a strongly electron withdrawing

nitro group in 4-position (AS-78) or the bulky electron donating phenoxy group (AS-85),

reduced PAP-1's selectivity. Again, without knowing the exact location of the binding site of the

PAPs on Kv1.3 and Kv1.5 it is hard to interpret these results, but it seems as if size is more

important than electronic effects in conferring selectivity over Kv1.5. In future studies we will

have to carefully map the binding site of the PAPs on Kv1.3. However, because of the chemical

similarity between PAP-1 and correolide it seems a valid first guess that it might be located in

the same area as the correolide binding site in the water filled inner cavity of Kv1.3 (Hanner et

al., 2001; Hanner et al., 1999). Although the two binding sites might overlap we expect that they

will not be identical. In contrast to the larger and more lipophilic nortriterpene correolide that

binds to Kv1.3 through the complementary shape between the bowl-like cavity wall and its own

surface, we expect that the PAPs will probably make fewer but "tighter" contacts on the channel

involving the two π-electron clouds of the side-chain phenyl ring and the psoralen moiety.

Another important difference between correolide and the PAPs consists in their stoichiometry of

interaction: correolide has a Hill coefficient of 1, while the PAPs exhibit Hill coefficients of 2.

We hypothesize that the PAPs bind in the lower region of S5-S6 and that two molecules "hook"

into the channel when the intracellular gate is wide open and lock the channel in the C-type

inactivated state.

PAP-1's good selectivity over other ion channels, receptors and transporters together with

its lack of cytotoxicity, mutagenicity, phototoxicity and acute toxicity in animals suggest that

PAP-1 might indeed be safe for *in vivo* use. Its low affinity to P450-dependent enzymes makes it

also unlikely that PAP-1 should cause any major drug-drug interactions that are mediated

through P450 inhibition. PAP-1 could therefore potentially constitute the first small molecule

that could be developed into a therapeutically useful immunomodulator. Based on its molecular weight of 350 and its logP value of 4.06, the Lipinski "rule of five" predicts that PAP-1 should be orally available and as our oral DTH experiments demonstrate that this is indeed the case. Compared to Psora-4, the additional O-atom in the linker did not only increase selectivity over Kv1.5 but also improved the solubility characteristics. While Psora-4 with a logP value of 4.33 was difficult to dissolve in aqueous solutions despite extensive use of solubilization aids such as ethanol, DMSO, Tween 80 or Cremophor, PAP-1's lower logP of 4.06 made it soluble in physiological saline with the addition of 25% Cremophor. PAP-1's detailed pharamacokinetics and tissue distribution will be the focus of future studies by our laboratory. These pharmacokinetic studies in combination with more detailed toxicity studies examining cardiac function will also help us to determine if the 23-fold selectivity over Kv1.5 is sufficient for safe *in vivo* use or if PAP-1's selectivity over Kv1.5 will have to be increased through further derivatization.

PAP-1 potently suppresses the activation of CCR7^{-} human T_{EM} cells in keeping with the previously described Kv1.3 dependence of these cells (Beeton et al., 2005; Wulff et al., 2003b). In contrast, PAP-1 is much less effective on naïve and T_{CM} cells demonstrating its relative selectivity for T_{EM} cells. Because of the crucial role of T_{EM} cells in the pathogenesis of the autoimmune diseases multiple sclerosis, type-1 diabetes, psoriasis, rheumatoid arthritis, and in transplant rejection as well as graft-versus host disease (Beeton and Chandy, 2005), PAP-1 constitutes an attractive new experimental drug for the treatment of these diseases. As a simple model of a T_{EM} cell mediated immune reaction we here used DTH and found that PAP-1 effectively prevented this reaction when administered intraperitoneally or orally.

In summary, we here describe the design of the first small molecule Kv1.3 blocker that is selective over the other Kv1-family channels. This selectivity and PAP-1's effectiveness in suppressing T_{EM} cells both *in vitro* and *in vivo*, make PAP-1 an ideal pharmacological tool to further evaluate Kv1.3 as a target for the prevention and treatment of autoimmune diseases in animal models of multiple sclerosis, type-1 diabetes, rheumatoid arthritis, transplant rejection and graft-versus-host disease. If proven effective in these models non-toxic in more detailed and more long-term toxicity tests, PAP-1 could potentially be developed into an orally available drug for the treatment of autoimmune diseases.

References

Averbeck D (1989) Recent advances in psoralen phototoxicity mechanism. *Photochem Photobiol* **50**:859-82.

Bardien-Kruger S, Wulff H, Arieff Z, Brink P, Chandy KG and Corfield V (2002) Characterization of the human voltage-gated potassium channel gene, KCNA7, a candidate gene for inherited cardiac disorders, and its exclusion as a cause of progressive familial heart block I (PFHBI). *Eur J Human Gen* **10**:36-43.

Beeton C, Barbaria J, Giraud P, Devaux J, Benoliel A, Gola M, Sabatier J, Bernard D, Crest M and Beraud E (2001a) Selective Blocking of Voltage-Gated K^+ Channels Improves Experimental Autoimmune Encephalomyelitis and Inhibits T Cell Activation. *J Immunol* **166**:936-944.

Beeton C and Chandy KG (2005) Potassium channels, memory T cells and multiple sclerosis. *Neuroscientist* in press.

Beeton C, Pennington MW, Wulff H, Singh S, Nugent D, Crossley G, Khaytin I, Calabresi PA, Chen CY, Gutman GA and Chandy KG (2005) Targeting effector memory T cells with a selective peptide inhibitor of Kv1.3 channels for therapy of autoimmune diseases. *Mol Pharmacol* **67**:1369-81.

Beeton C, Wulff H, Barbaria J, Clot-Faybesse O, Pennington M, Bernard D, Cahalan MD, Chandy KG and Beraud E (2001b) Selective Blockade of T lymphocyte K^+ channels ameliorates experimental autoimmune encephalomyelitis, a model for multiple sclerosis. *Proc Natl Acad Sci USA* **98**:13942-13947.

Bohuslavizki HK, Hinck-Kneip C, Kneip A, Koppenhofer E and Reimers A (1993) Reduction of MS-related scotoma by a new class of potassium channel blockers from Ruta graveolens. *Neuroopthalmol* **13**:191-198.

Bohuslavizki KH, Hansel W, Kneip A, Koppenhofer E, Niemoller E and Sanmann K (1994) Mode of action of psoralens, benzofurans, acridones and coumarins on the ionic currents in intact myelinated nerve fibres and its significance in demyelinating diseases. *Gen. Physiol. Biophys.* **13**:309-328.

Cahalan MD, Chandy KG, DeCoursey TE and Gupta S (1985) A voltage-gated potassium channel in human T lymphocytes. *J Physiol (Lond)* **358**:197-237.

Chandy KG, Wulff H, Beeton C, Pennington M, Gutman GA and Cahalan MD (2004) Potassium channels as targets for specific immunomodulation. *Trends Pharmacol Sci* **25**:280-289.

Dall' Acqua F, Marciani S, Ciavetta L and Rodighiero G (1971) Formation of inter-strand cross-links in the photoreactions between furocoumarins and DNA. *Z. Naturforsch.* **26b**:561-569.

Dorner T and Lipsky PE (2004) Correlation of circulating CD27high plasma cells and disease activity in systemic lupus erythematosus. *Lupus* **13**:283-289.

Fasth AE, Cao D, van Vollenhoven R, Trollmo C and Malmstrom V (2004) CD28nullCD4+ T cells--characterization of an effector memory T-cell population in patients with rheumatoid arthritis. *Scand J Immunol* **60**:199-208.

Fedida D, Wible B, Wang Z, Fermini B, Faust F, Nattel S and Brown A (1993) Identity of a novel delayed rectifier current from human heart with a cloned K^+ channel current. *Circ Res* **73**:210-216.

Gasparro FP (2000) The role of PUVA in the treatment of psoriasis. Photobiology issues related to skin cancer incidence. *Am J Clin Dermatol* **1**:337-48.

Grissmer S, Dethlefs B, Wasmuth JJ, Goldin AL, Gutman GA, Cahalan MD and Chandy KG (1990) Expression and chromosomal localization of a lymphocyte K$^+$ channel gene. *Proc Natl Acad Sci U S A* **87**:9411-9415.

Grissmer S, Nguyen AN, Aiyar J, Hanson DC, Mather RJ, Gutman GA, Karmilowicz MJ, Auperin DD and Chandy KG (1994) Pharmacological characterization of five cloned voltage-gated K$^+$ channels, types Kv1.1, 1.2, 1.3, 1.5, and 3.1, stably expressed in mammalian cell lines. *Mol. Pharmacol.* **45**:1227-1234.

Gutman GA, Chandy KG, Adelman JP, Aiyar J, Bayliss DA, Clapham DE, Covarriubias M, Desir GV, Furuichi K, Ganetzky B, Garcia ML, Grissmer S, Jan LY, Karschin A, Kim D, Kuperschmidt S, Kurachi Y, Lazdunski M, Lesage F, Lester HA, McKinnon D, Nichols CG, O'Kelly I, Robbins J, Robertson GA, Rudy B, Sanguinetti M, Seino S, Stuehmer W, Tamkun MM, Vandenberg CA, Wei A, Wulff H and Wymore RS (2003) International Union of Pharmacology. XLI. Compendium of voltage-gated ion channels: potassium channels. *Pharmacol Rev* **55**:583-586.

Hanner M, Green B, Gao Y-D, Schmalhofer W, Matyskiela M, Durand DJ, Felix JP, Linde A-R, Bordallo C, Kaczorowski GJ, Kohler M and Garcia ML (2001) Binding of correolide to the Kv1.3 potassium channel: characterization of the binding domain by site-directed mutagenesis. *Biochemistry* **40**:11687-11697.

Hanner M, Schmalhofer WA, Green B, Bordallo C, Liu J, Slaughter RS, Kaczorowski GJ and Garcia ML (1999) Binding of correolide to Kv1 family potassium channels. *J Biol Chem* **274**:25237-25244.

Hansen A, Odendahl M, Reiter K, Jacobi AM, Feist E, Scholze J, Burmester GR, Lipsky PE and Dorner T (2002) Diminished peripheral blood memory B cells and accumulation of

memory B cells in the salivary glands of patients with Sjogren's syndrome. *Arthritis Rheum* **46**:2160-71.

Hanson DC, Nguyen A, Mather RJ, Rauer H, Koch K, Burgess LE, Rizzi JP, Donovan CB, Bruns MJ, Canniff PC, Cunningham AC, Verdries KA, Mena E, Kath JC, Gutman GA, Cahalan MD, Grissmer S and Chandy KG (1999) UK-78,282, a novel piperidine compound that potently blocks the Kv1.3 voltage-gated potassium channel and inhibits human T cell activation. *Br J Pharmacol* **126**:1707-16.

Henderson GL, Harkey MR, Gershwin ME, Hackman RM, Stern JS and Stressser DM (1999) Effects of gingseng components on c-DNA-expressed cytochrome P450 enzyme catalytic activity. *Life Sci.* **65**:PL209-214.

Kolski-Andreaco A, Tomita H, Shakkottai VG, Gutman GA, Cahalan MD, Gargus JJ and Chandy KG (2004) SK3-1C, a dominant-negative suppressor of SKCa and IKCa channels. *J Biol Chem* **279**:6893-904.

Kraljic I and El Moshnie SE (1978) A new method for the detection of singlet oxygen in aqueous solution. *Photochem Photobiol* **28**:577-581.

Levy DI and Deutsch C (1996) Recovery from C-type inactivation is modulated by extracellular potassium. *Biophys J* **70**:798-805.

Lipinski CA, Lombardo F, Dominy BW and Feeney PJ (1997) Experimental and computational approaches to estimate solubility and permeability in drug discovery and development settings. *Adv Drug Delivery Rev* **23**:3-25.

Markovic-Plese S, Cortese I, Wandinger KP, McFarland HF and Martin R (2001) CD4^{+}CD28^{-} costimulation-independent T cells in multiple sclerosis. *J Clin Invest* **108**:1185-1194.

Nguyen A, Kath JC, Hanson DC, Biggers MS, Canniff PC, Donovan CB, Mather RJ, Bruns MJ, Rauer H, Aiyar J, Lepple-Wienhues A, Gutman GA, Grissmer S, Cahalan MD and Chandy KG (1996) Novel nonpeptide agents potently block the C-type inactivated conformation of Kv1.3 and suppress T cell activation. *Mol Pharmacol* **50**:1672-1679.

Panyi G, Sheng Z and Deutsch C (1995) C-type inactivation of a voltage-gated K+ channel occurs by a cooperative mechanism. *Biophys J* **69**:896-903.

Pearl JP, Parris J, Hale DA, Hoffmann SC, Bernstein WB, McCoy KL, Swanson SJ, Mannon RB, Roederer M and Kirk AD (2005) Immunocompetent T-cells with a memory-like phenotype are the dominant cell type following antibody-mediated T-cell depletion. *Am J Transplant* **5**:465-74.

Ross PE, Garber SS and Cahalan MD (1994) Membrane Chloride Conductance and Capcitance in Jurkat T Lymphocytes during Osmotic Swelling. *Biophys J* **66**:169-178.

Sage E and Moustacchi E (1987) Sequence context effects on 8-methoxypsoralen photobinding to defined DNA fragments. *Biochemistry* **26**:3307-3314.

Schmalhofer WA, Bao J, McManus OB, Green B, Matyskiela M, Wunderler D, Bugianesi RM, Felix JP, Hanner M, Linde-Arias A-R, Ponte CG, Velasco L, Koo G, Staruch MJ, Miao S, Parsons WH, Rupprecht K, Slaughter RS, Kaczorowski GJ and Garcia ML (2002) Identification of a new class of inhibitors of the voltage-gated potassium channel, Kv1.3, with immunosuppressant properties. *Biochemistry* **18**:7781-7794.

Schoenberg A and Aziz G (1953) Furochromones and Coumarins. VI. Demethylation of xanthotoxin, khellin and khellol with aniline hydrochloride and magnesium iodide. *Am J Chem Soc* **75**:3265-3266.

Singh SB, Zink DL, Dombrowski AW, Dezeny G, Bills GF, Felix JP, Slaughter RS and Goetz MA (2001) Candelalides A-C: novel diterpenoid pyrones from fermentations of Sesquicillium candelabrum as blockers of the voltage-gated potassium channel Kv1.3. *Org Lett* **3**:247-350.

Soler D, Humphreys TL, Spinola SM and Campbell JJ (2003) CCR4 versus CCR10 in human cutaneous TH lymphocyte trafficking. *Blood* **101**:1677-1682.

Vedaldi D, Caffieri S, Frank S, Dall'Acqua F, Jakobs A and Piette J (1995) Sulphur and selenium analogues of psoralen as novel potential photochemotherapeutic agents. *Farmaco* **50**:527-536.

Vennekamp J, Wulff H, Beeton C, Calabresi PA, Grissmer S, Hansel W and Chandy KG (2004) Kv1.3 blocking 5-phenylalkoxypsoralens: a new class of immunomodulators. *Mol Pharmacol* **65**:1364-1373.

Viglietta V, Kent SC, Orban T and Hafler DA (2002) GAD65-reactive T cells are activated in patients with autoimmune type 1a diabetes. *J Clin Invest* **109**:895-903.

Vissers WH, Arndtz CH, Muys L, Van Erp PE, de Jong EM and van de Kerkhof PC (2004) Memory effector (CD45RO+) and cytotoxic (CD8+) T cells appear early in the margin zone of spreading psoriatic lesions in contrast to cells expressing natural killer receptors, which appear late. *Br J Dermatol* **150**:852-9.

Wermuth CG (2004) Selective optimization of side activities: another way for drug discovery. *J Med Chem* **47**:1303-14.

Wernekenschnieder A, Korner P and Hansel W (2004) 3-Alkyl- and 3-aryl-7H-furo[3,2-g]chromen-7-ones as blockers of the voltage-gated potassium channel Kv1.3. *Pharmazie* **59**:319-20.

Wulff H, Beeton C and Chandy KG (2003a) Potassium channels as therapeutic targets for autoimmune disorders. *Curr Opin Drug Discovery & Development* **6**:640-647.

Wulff H, Calabresi PA, Allie R, Yun S, Pennington M, Beeton C and Chandy KG (2003b) The voltage-gated Kv1.3 K$^+$ channel in effector memory T cells as new target for MS. *J Clin Invest* **111**:1703-1713.

Wulff H, Knaus HG, Pennington M and Chandy KG (2004) K$^+$ channel expression during B-cell differentiation: implications for immunomodulation and autoimmunity. *J Immunol* **173**:776-786.

Wulff H, Miller MJ, Haensel W, Grissmer S, Cahalan MD and Chandy KG (2000) Design of a potent and selective inhibitor of the intermediate-conductance Ca^{2+}-activated K$^+$ channel, IKCa1: A potential immunosuppressant. *Proc Natl Acad Sci USA* **97**:8151-8156.

Wulff H, Rauer H, During T, Hanselmann C, Ruff K, Wrisch A, Grissmer S and Haensel W (1998) Alkoxypsoralens, novel nonpeptide blockers of Shaker-type K$^+$ channels: synthesis and photoreactivity. *J Med Chem* **41**:4542-9.

Yamashita K, Choi U, Woltz PC, Foster SF, Sneller MC, Hakim FT, Fowler DH, Bishop MR, Pavletic SZ, Tamari M, Castro K, Barrett AJ, Childs RW, Illei GG, Leitman SF, Malech HL and Horwitz ME (2004) Severe Chronic Graft-Versus-Host Disease is Characterized by a Preponderance of CD4$^+$ Effector Memory Cells Relative to Central Memory Cells. *Blood* **103:**3986-3988.

Zarebska Z (1994) Cell membrane, a target for PUVA therapy. *J Photochem Photobiol B* **23**:101-109.

MOLPHARM/2005/15669

Zhang W, Kilicarslan T, Tyndale RF and Sellers EM (2001) Evaluation of methoxsalen, tranylcypromine, and tryptamine as specific and selective CYP2A6 inhibitors in vitro. *Drug Metab Dispos* **29**:897-902.

Zhou Z, Gong Q, Ye B, Fan Z, Makielski JC, Robertson GA and January CT (1998) Properties of HERG channels stably expressed in HEK 293 cells studied at physiological temperatures. *Biophys J* **74**:230-241.

Footnotes

Legends for Figures

Fig. 1. A, *Ruta graveolens* was the source of 5-MOP, which served as a template for the Kv1.3

blocker Psora-4. B, Design strategy for new Psora-4 analogs.

Fig. 2. *Top,* EC_{50} values of compounds synthesized under strategy-a (see Fig.1B for chemical

structures). *Middle,* Chemical structures and EC_{50} values of compounds from strategy-b. Bottom,

EC_{50} values and structures of compounds that were synthesized through a combination of

strategies b + c. All compound were tested three to five times at four to six concentrations and

EC_{50} values were determined by fitting the Hill equation to the reduction of area under the

current curve at 40 mV. The standard deviations were smaller than 10% in each case.

Fig. 3. A, Inhibition of Kv1.3 current by increasing concentrations of PAP-1 in a L929 cell

stably expressing Kv1.3. For each concentration equilibrium block after 15 pulses is shown. B,

Concentration-response curve for PAP-1 on Kv1.3. Each concentration was tested at least three

times. C, EC_{50} values of PAP-1 on a panel of 22 cloned and native K^+, Na^+, Ca^{2+} and Cl^-

channels. PAP-1 was tested at three to five concentrations on each channel (n = 3).

Fig. 4. A, Pulse protocol for experiments shown in B. Kv1.3 currents were elicited by a 200-ms

depolarizing pulse to 40 mV. PAP-1 (10 nM) was applied to the bath while the membrane was

held at −80 mV. After an interval of 5 min, consecutive 2 ms, 200 ms or 2-sec pulses were

applied every 60 sec. B, Inhibition of Kv1.3 by 10 nM PAP-1 during consecutive 200-ms (*left*)

or 2-sec pulses (*right*). The numbers 1-15 refer to pulses 1-15. C, Effect of varying the pulse

length from 2 ms to 2 sec on time to reach steady state block. Ordinate: ratio of area under the

current curve at various times after start of the consecutive pulses to current before PAP-1 application (n = 3). D, Kv1.3 was driven into the C-type inactivated state by 5 rapid pulses at an interval of 1 sec. This pulse protocol was repeated 5 min later to assure that the channel ensemble completely recovered from inactivation in 5 min. PAP-1 (10 nM) was then immediately perfused onto the inactivated channels. After 5 min we repeated the same rapid pulse protocol. E, Effect of changing the external K^+ concentration on the potency of PAP-1 to block WT Kv1.3. Shown are steady state currents 15 pulses after drug application. F, Effect of the H339T mutation in Kv1.3 on the potency of PAP-1.

Fig. 5. A, Effect of PAP-1 on the anti-CD3 Ab stimulated proliferation of human CCR7$^-$ T$_{EM}$ cells (*left*) and PBMCs (*right*). Shown are means ± SD from one representative experiment. B, Dose-dependent inhibition of DTH reaction by i.p. administration of PAP-1. Shown are the pooled means ± SEM of differences in ear thickness before and 24 hours after the challenge from two independent experiments. Vehicle (250 μl PBS containing 25% cremophor EL), PAP-1 or ShK (16 μg/kg) were injected i.p. 3x daily for 48 hours. The difference in ear thickness between control (n = 10) and 0.3 mg/kg PAP-1 (n = 8) is not statistically significant (p = 0.13). All other effects are statistically significant: control versus 1.0 mg/kg PAP-1 (n = 7) p= 0.001; control versus 3.0 mg/kg PAP-1 (n = 8) p = 0.00008; control versus ShK (n = 3) p = 0.0009. At 3 mg/kg PAP-1 is not statistically different from ShK (p = 0.06). C, Dose-dependent inhibition of DTH by PAP-1 administered in 500 μl peanut oil by gavage. Shown are the means ± SEM from one experiment. The difference in ear thickness between control (n = 4) and 5 mg/kg PAP-1 (n = 4) is not statistically significant (p = 0.12). All other effects are statistically significant: control versus 20 mg/kg PAP-1 (n = 3) p = 0.035; control versus 80 mg/kg PAP-1 (n = 3) p = 0.00003.

Tables

Compound	CYP2A6 (IC$_{50}$ μM)	CYP3A4 (IC$_{50}$ μM)
PAP-1	46 ± 7	2.35 ± 0.07
AS-78	> 200	5.45 ± 0.08
AS-77	2.1 ± 0.1	> 200
PH-9	15 ± 1.4	14.5 ± 0.1
5-MOP	>200	6.85 ± 0.07
Positive control	0.17 ± 0.04	0.037 ± 0.005

Table 1. Inhibition of CYP2A6 and CYP3A4 by selected psoralens. The positive controls were tranylcypromine (CYP2A6) and ketoconazole (CYP3A4).
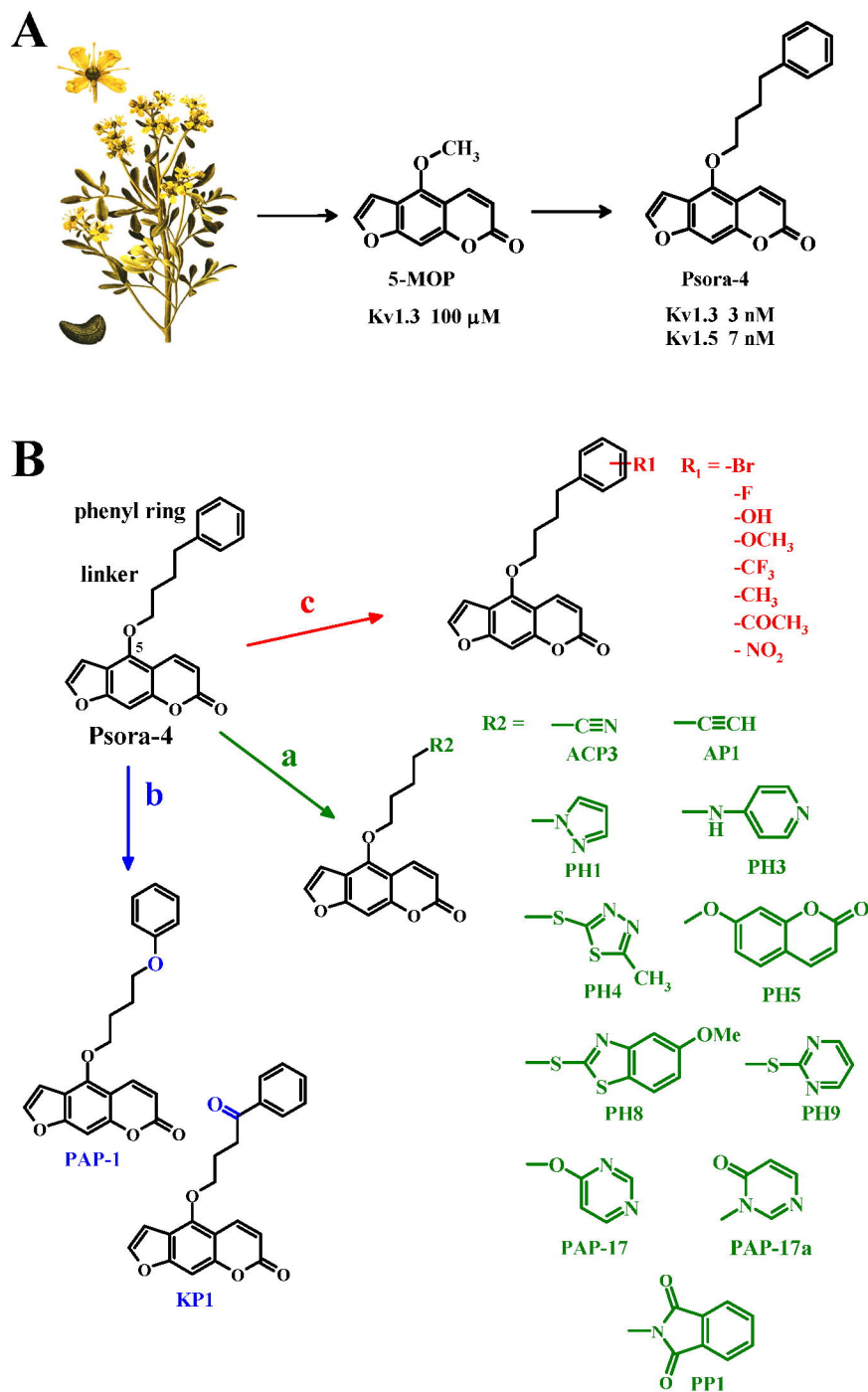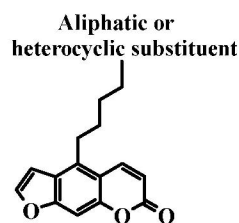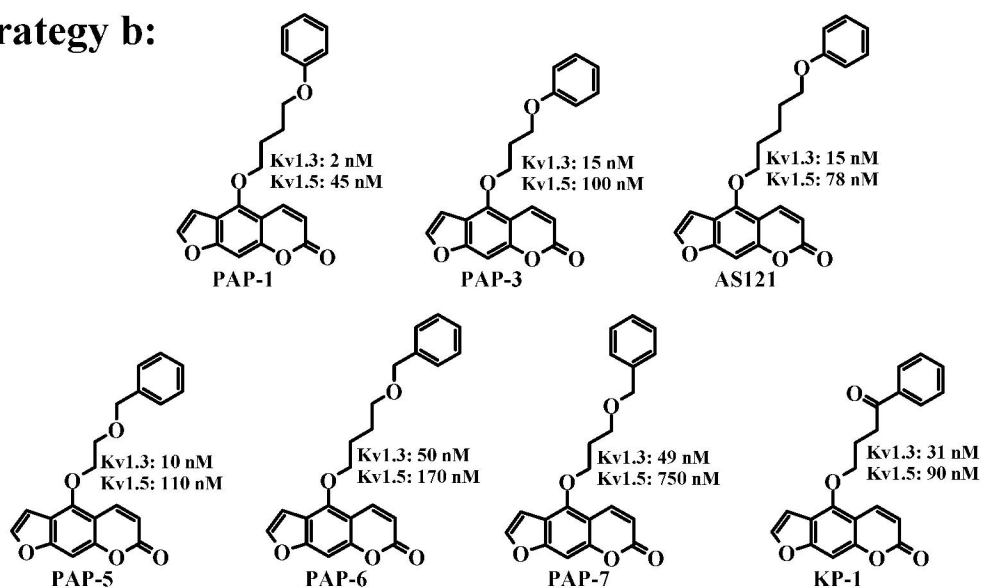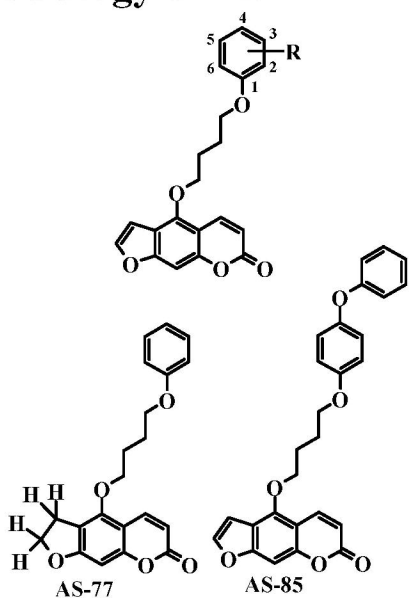
Figure 1

Strategy a:

Aliphatic or heterocyclic substituent

	EC$_{50}$ Kv1.3	EC$_{50}$ Kv1.5
ACP-3	1.3 μM	5 μM
AP-1	280 nM	500 nM
PH-1	450 nM	5 μM
PH-3	5 μM	5 μM
PH-4	175 nM	5 μM
PH-5	125 nM	5 μM
PH-8	35 nM	100 nM
PH-9	50 nM	159 nM
PAP-17	125 nM	425 nM
PAP-17a	7 μM	>5 μM
PP-1	450 nM	900 nM

Strategy b:

Kv1.3: 2 nM
Kv1.5: 45 nM
PAP-1

Kv1.3: 15 nM
Kv1.5: 100 nM
PAP-3

Kv1.3: 15 nM
Kv1.5: 78 nM
AS121

Kv1.3: 10 nM
Kv1.5: 110 nM
PAP-5

Kv1.3: 50 nM
Kv1.5: 170 nM
PAP-6

Kv1.3: 49 nM
Kv1.5: 750 nM
PAP-7

Kv1.3: 31 nM
Kv1.5: 90 nM
KP-1

Strategy b + c:

AS-77

AS-85

	R	EC$_{50}$ Kv1.3	EC$_{50}$ Kv1.5
AS-67	4-OCH$_3$	8 nM	10 nM
AS-68	3-OCH$_3$	18 nM	45 nM
AS-69	3,5-(OCH$_3$)$_2$	120 nM	150 nM
AS-96	4-CH$_3$	7 nM	20 nM
AS-118	3-CF$_3$	65 nM	250 nM
AS-111	4-F	12 nM	12 nM
AS-84	4-Cl	5 nM	10 nM
AS-78	4-NO$_2$	5 nM	105 nM
PAP-12	2-NO$_2$	61 nM	244 nM
PAP-13	3-NO$_2$	81 nM	90 nM
PAP-14	2,4-(NO$_2$)$_2$	140 nM	297 nM
PAP-10	2-OCH$_3$, 4-NO$_2$	500 nM	476 nM
PAP-11	2-NO$_2$, 4-CH$_3$	700 nM	248 nM
AS-85		16 nM	750 nM
AS-77		22 nM	45 nM

Figure 2

A

B

$n_H = 1.8$

PAP-1

C

	EC$_{50}$ [nM]		EC$_{50}$ [nM]
Kv1.1	65 ± 8	**Kv11.1**	5000 ± 1000
Kv1.2	250 ± 14	**Kir2.1**	15 000 ± 1000
Kv1.3	2.0 ± 0.2	**KCa1.1**	2500 ± 500
Kv1.4	75 ± 5	**KCa2.1**	10 000 ± 1000
Kv1.5	45 ± 3	**KCa2.2**	5000 ± 1000
Kv1.6	62 ± 3	**KCa2.3**	5000 ± 1000
Kv1.7	98 ± 5	**KCa3.1**	10 000 ± 1000
Kv2.1	3000 ± 500	**Nav1.2**	7000 ± 1000
Kv3.1	5000 ± 1000	**Nav1.4**	7000 ± 1000
Kv3.2	980 ± 50	**Cav1.2**	5000 ± 1000
Kv4.2	1200 ± 100	**Cl$^-_{swell}$**	15 000 ± 1000

Figure 3

Figure 4

Figure 5